CANCER

RNA binding protein PCBP1 is an intracellular immune checkpoint for shaping T cell responses in cancer immunity

Ephraim A. Ansa-Addo[1,2*†], Huai-Cheng Huang[1,3*], Brian Riesenberg[1,2], Supinya Iamsawat[1], Davis Borucki[1], Michelle H. Nelson[1], Jin Hyun Nam[4], Dongjun Chung[2,4‡], Chrystal M. Paulos[1§], Bei Liu[1], Xue-Zhong Yu[1], Caroline Philpott[5], Philip H. Howe[6], Zihai Li[1,2†]

Copyright © 2020 The Authors, some rights reserved; exclusive licensee American Association for the Advancement of Science. No claim to original U.S. Government Works. Distributed under a Creative Commons Attribution NonCommercial License 4.0 (CC BY-NC).

Distinct lineages of T cells can act in response to various environmental cues to either drive or restrict immune-mediated pathology. Here, we identify the RNA binding protein, poly(C)-binding protein 1 (PCBP1) as an intracellular immune checkpoint that is up-regulated in activated T cells to prevent conversion of effector T (T_{eff}) cells into regulatory T (T_{reg}) cells, by restricting the expression of T_{eff} cell–intrinsic T_{reg} commitment programs. This was critical for stabilizing T_{eff} cell functions and subverting immune-suppressive signals. T cell–specific deletion of *Pcbp1* favored T_{reg} cell differentiation, enlisted multiple inhibitory immune checkpoint molecules including PD-1, TIGIT, and VISTA on tumor-infiltrating lymphocytes, and blunted antitumor immunity. Our results demonstrate a critical role for PCBP1 as an intracellular immune checkpoint for maintaining T_{eff} cell functions in cancer immunity.

INTRODUCTION

Immune checkpoint blockade (ICB) with antibodies targeting coinhibitory molecules programmed cell death-1 (PD-1) and cytotoxic T-lymphocyte associated protein 4 (CTLA-4) have demonstrated clinical benefits in malignances such as melanoma, non–small cell lung, and cancer head and neck cancer, ultimately changing the practice of medical oncology (*1*–*4*). ICB has particularly been successful in melanoma, where up to 40% of patients show evidence of continued durable disease control. Recent evidence, which suggests that blocking one inhibitory receptor allows another to dominate and subvert antitumor immunity, provides further impetus for combination therapy or dual blockade of immune checkpoint to improve response and survival (*1*, *5*). However, there are considerable toxicities associated with this approach, and therefore, optimizing treatments to define responders versus nonresponders is pertinent. Moreover, identifying additional molecular predictors of response to ICB would support more robust predictions and improve treatment outcomes in patients (*6*, *7*).

RNA binding proteins (RBPs) are important posttranscriptional regulators that control RNA biology (splicing, stability, etc.) and translation. RBPs also enable T cells to maintain a poised transcriptome that can be rapidly translated in response to T cell receptor (TCR) stimulation. Thus, RBPs are quickly emerging as critical regulators of gene expression in response to T cell activation and differentiation (*8*–*10*). One such RBP is the poly(C)-binding proteins (PCBPs), which are multifunctional adaptor proteins implicated in the regulation of numerous biological processes. Most cell types express PCBP1, a member of a family of four homologous proteins that includes PCBP2, PCBP3, and PCBP4 (*11*). Besides RNA binding, PCBP1 also functions as an iron-binding protein that delivers iron to ferritin and other iron-dependent proteins (*12*, *13*). Moreover, PCBP1 exhibits DNA and RNA binding properties, as well as controlling protein output by altering the fate of their binding targets (*14*, *15*). Notably, the RNA binding function of PCBP1 is regulated by the phosphorylation state of the protein (*16*, *17*). That is, unphosphorylated PCBP1 is able to bind to selective mRNAs and restrict their translation, thereby repressing its targets. However, in a chronic immune-suppressive setting, such as cancer, PCBP1 is phosphorylated at Ser^{43} by transforming growth factor–β (TGF-β) via the protein kinase, Bβ/AKT2, causing release of PCBP1 from the target transcript and subsequent mRNA translation, thus derepression of targets (*18*–*20*). Notably, the liberated mRNAs subsequently regulate downstream transcription. One such target, moesin, is repressed by PCBP1 in activated T cells but is posttranscriptionally induced in regulatory T cells (T_{regs}) via TGF-β–mediated release from PCBP1 repression (*21*). In turn, moesin promotes optimal TGF-β signaling by stabilizing the TGF-β receptors, which consequently augments T_{reg} differentiation (*21*). Although PCBP1 was recently reported to promote granulocyte-macrophage colony-stimulating factor (GM-CSF) production by T cells (*22*), the physiological roles of PCBP1 in the development and function of $CD4^+$ and $CD8^+$ T cells, as well as T_{reg} differentiation, are unknown. Because of its sensitivity to TGF-β signaling, inhibition of PCBP1 function may be a critical strategy for tumors to subvert antitumor immunity.

Here, we found that PCBP1 is up-regulated in activated T cells. PCBP1 was critical for stabilizing effector T cell functions by preventing their shift into T_{regs} and subverting immune-suppressive signals. Specifically, PCBP1 constrained expression of effector T cell–intrinsic T_{reg} commitment programs to safeguard the immune response and antitumor functions. Consequently, T cell–specific

[1]Department of Microbiology and Immunology and Hollings Cancer Center, Medical University of South Carolina, Charleston, SC 29425, USA. [2]Pelotonia Institute for Immuno-Oncology and Division of Medical Oncology, Department of Internal Medicine, The Ohio State University Comprehensive Cancer Center-James, Columbus, OH 43210, USA. [3]National Taiwan University College of Medicine, Graduate Institute of Clinical Medicine, No.7 Chung San South Road, Taipei City 10002, Taiwan. [4]Department of Public Health Sciences, Medical University of South Carolina, Charleston, SC 29425, USA. [5]Genetics and Metabolism Section, Liver Diseases Branch, National Institute of Diabetes and Digestive and Kidney Diseases (NIDDK), Bethesda, MD 20892, USA. [6]Department of Biochemistry and Molecular Biology, Medical University of South Carolina, Charleston, SC 29425, USA.
*These authors contributed equally to this work.
†Corresponding author. Email: ephraim.ansa-addo@osumc.edu (E.A.A.-A); zihai.li@osumc.edu (Z.L.)
‡Present address: Department of Biomedical Informatics, The Ohio State University, Columbus, OH 43210, USA.
§Present address: Department of Surgery and Department of Microbiology and Immunology, Winship Cancer Institute, Emory University School of Medicine, Atlanta, GA 30322, USA.

deletion of PCBP1 resulted in a significantly greater proportion of forkhead box protein P3–positive (FoxP3$^+$) T_{regs} that alleviated acute graft-versus-host disease (aGVHD) but blunted antitumor responses in mice. Whole-transcriptome analysis revealed that PCBP1 has a global function in restricting the expression of genes that promote immune tolerance.

RESULTS

PCBP1 is up-regulated in activated T cells

To gain insight into the role of PCBP1 in T cells, we first analyzed the expression of mRNA encoding members of the PCBP family in human CD3$^+$ T cells before and after activation (*23*). We found that *PCBP1* mRNA was abundant in both resting T cells and in activated T cells (Fig. 1A). We next assessed PCBP1 protein expression in naïve/resting (T0 and Tc-0) or anti-CD3/anti-ICOS paramagnetic activated (Th0 and Tc-1) human T cells from healthy individuals. We detected lower PCBP1 expression in naïve CD4$^+$ (Fig. 1B) and CD8$^+$ (Fig. 1C) T cells that was robustly up-regulated upon bead activation. Moesin, which is repressed by PCBP1 (*21*), was also elevated in resting T cells but was rapidly down-regulated in activated human T cells (Fig. 1, B and C).

PCBP1 levels in ex vivo mouse splenic lymphocytes were grossly comparable (Fig. 1D). Similar to human T cells, *Pcbp1* mRNA was comparable between resting and activated mouse T cells but increased in iT_{regs} (Fig. 1E). PCBP1 protein was markedly elevated in CD4$^+$ and CD8$^+$ T cells after TCR stimulation (Fig. 1, F to J). In addition, PCBP1 was distinctly expressed in CD69^{low} and CD69^{high} CD8$^+$ T cells cultured in vitro with increasing doses of interleukin-2 (IL-2) (fig. S1, A to E). Consistent with PCBP1 repression of moesin translation (*21*), PCBP1 was reduced in unstimulated T cells with a concomitant increase of moesin in CD4$^+$ (Fig. 1, G and H) and CD8$^+$ T cells (Fig. 1, I and J) isolated from the spleen of wild-type (WT) mice. Activation of T cells up-regulated PCBP1, which then repressed moesin expression (Fig. 1, G to J) (*21*). iT_{reg} differentiation rescued moesin expression (Fig. 1, G and H) because of TGF-β–mediated phosphorylation of PCBP1, which abrogates its repressive function (Fig. 1, K and L, and fig. S1, F and G) (*18*, *21*). These results indicated that PCBP1 is rapidly up-regulated in response to T cell activation to restrict translation of moesin. Because of the rapid induction of PCBP1 in activated T cells and elevated mRNA in early thymocytes (fig. S1H), we wondered whether PCBP1 has a cell-autonomous role in T cells.

PCBP1 inhibits optimal differentiation of T_{regs}

We next sought to examine the physiological roles of PCBP1 in T cells; we mated mice with *lox*P-flanked alleles (*Pcbp1*$^{f/f}$) (*12*) to mice with transgenic expression of Cre recombinase from the T cell–specific *Cd4* promoter (*Cd4*-Cre) to generate *Pcbp1*$^{f/f}$*Cd4*-Cre progeny. Notably, *Pcbp1*-null embryos are rendered nonviable in the peri-implantation stage (*24*). We confirmed efficient deletion of *Pcbp1* in single-positive (SP) CD4 and CD8, but not in double-negative (DN) thymocytes, by flow cytometry (fig. S2A). We found that *Pcbp1*$^{fl/fl}$*Cd4*-Cre mice exhibited a lower frequency of SP4 and SP8 cells that resulted in greater than twofold fewer matured thymocytes, although the total number of thymocytes and double-positive cells was unaltered relative to control mice (fig. S2B). As expected, the frequency of DN thymocytes was unaltered in *Pcbp1*$^{f/f}$*Cd4*-Cre mice compared to WT littermates (fig. S2C); however, the proportion of SP4 FoxP3$^+$CD25$^+$ mature thymic T_{regs} (tT_{regs}), as well as T_{reg} precursor cells (pre-T_{regs}; SP4 CD25$^+$GITR$^+$FoxP3$^-$) (*25*), was increased in *Pcbp1*$^{fl/fl}$*Cd4*-Cre mice (fig. S2, D and E). A similar reduction of matured T cells was observed in the spleen and lymph nodes of *Pcbp1*$^{fl/fl}$*Cd4*-Cre mice (fig. S2, F to H). Notably, *Pcbp1*$^{fl/fl}$*Cd4*-Cre mice appeared normal and do not exhibit any lymphoproliferative or myeloproliferative disorders. We next examined FoxP3$^+$ T_{reg} subsets in the thymus and peripheral lymphoid organs of *Pcbp1*$^{fl/fl}$*Cd4*-Cre and WT littermates. As observed in vitro, *Pcbp1*$^{fl/fl}$*Cd4*-Cre mice contained significantly greater frequencies and absolute number of FoxP3$^+$ T_{regs} in the thymus and peripheral organs (Fig. 2, A and B). Moreover, T_{regs} in *Pcbp1*$^{fl/fl}$*Cd4*-Cre mice expressed elevated CD25, GITR, and NRP1 (fig. S3A); however, CTLA-4 and KLRG-1 were reduced, and Helios expression was unchanged (fig. S3B).

We sought to determine why FoxP3$^+$ T_{regs} are increased in *Pcbp1*$^{fl/fl}$*Cd4*-Cre mice. We reasoned that induction of PCBP1 by T cell activation is critical to restrict the expression of T_{reg} commitment molecules, thus preventing activated T cells from differentiating toward immunosuppressive T_{regs} while stabilizing the functions of effector T cells. If so, then deleting PCBP1 from T cells would shift the balance toward increased development of FoxP3$^+$ T_{regs} (Fig. 2, A and B, and fig. S2D). We examined the proportion of FoxP3$^+$ T_{regs} that express the tT_{reg} commitment molecules Helios, NRP1, and CD25 (*26*–*28*). As expected, the frequencies of FoxP3$^+$CD25$^+$ matured T_{regs}, as well as Helios (Foxp3$^+$Helios^{high})– and NRP1-expressing (FoxP3$^+$NRP1^{high}) cells, were increased in the spleen of *Pcbp1*$^{fl/fl}$*Cd4*-Cre mice compared to littermate controls (Fig. 2C). The proportion of FoxP3$^-$CD25$^+$, FoxP3$^-$Helios^{high}, and FoxP3$^-$NRP1^{high} cells within the CD4$^+$FoxP3$^-$ T cell population was notably increased in *Pcbp1*$^{fl/fl}$*Cd4*-Cre mice (Fig. 2D), suggesting a poised state in knockout (KO) T cells that potentially supports rapid shift to the T_{reg} lineage in response to TCR signaling. Further analysis revealed a lower frequency of CD4$^+$CD44^{hi}CD62L^{lo} (Fig. 2E) but unexpectedly greater fraction of CD8$^+$CD44^{hi}CD62L^{lo} (Fig. 2F) effector memory T cells in the periphery of *Pcbp1*$^{fl/fl}$*Cd4*-Cre mice relative to WT. Nonetheless, PCBP1-deficient mice had fewer interferon-γ (IFN-γ) and tumor necrosis factor–α (TNF-α)–producing splenic T cells (Fig. 2, G and H). These data suggested that PCBP1 is crucial for maintaining peripheral T cell homeostasis and CD4$^+$ T cells in *Pcbp1*$^{fl/fl}$*Cd4*-Cre mice are less activated with reduced functionality.

Despite the decreased T cell functionality and increased T_{regs}, there was no difference in the frequency of CD4$^+$FoxP3$^-$ T cells expressing the transcription factors Tbet, GATA3, and RORγt, which are master transcription factors expressed in T helper 1 (T_H1), T_H2, and T_H17, respectively (fig. S3, C and D). Together, these findings suggest an essential role for PCBP1 in stabilizing the function of effector T cells, as well as maintaining peripheral T cell homeostasis by limiting conversion to T_{regs} in response to TCR signaling.

PCBP1 expression is not essential for the maintenance of T_{regs}

Next, we sought to address the role of PCBP1 specifically in T_{regs}. We deleted *Pcbp1* in differentiated T_{regs} from the FoxP3$^+$ tT_{reg} cell stage onwards by generating *Pcbp1*$^{fl/fl}$*Foxp3*-Cre$^+$ mice. These mice did not show any major changes in T_{reg} signature molecules, which indicates that PCBP1 is not required for the maintenance of T_{regs} (fig. S4A). We also generated chimeric female mice that were homozygous for the floxed *Pcbp1* allele and heterozygous for *Foxp3*$^{YFP\text{-}Cre}$ [PCBP1 chimeric KO mice; yellow fluorescent protein (YFP) marks cells with active Cre recombinase]. Following random inactivation

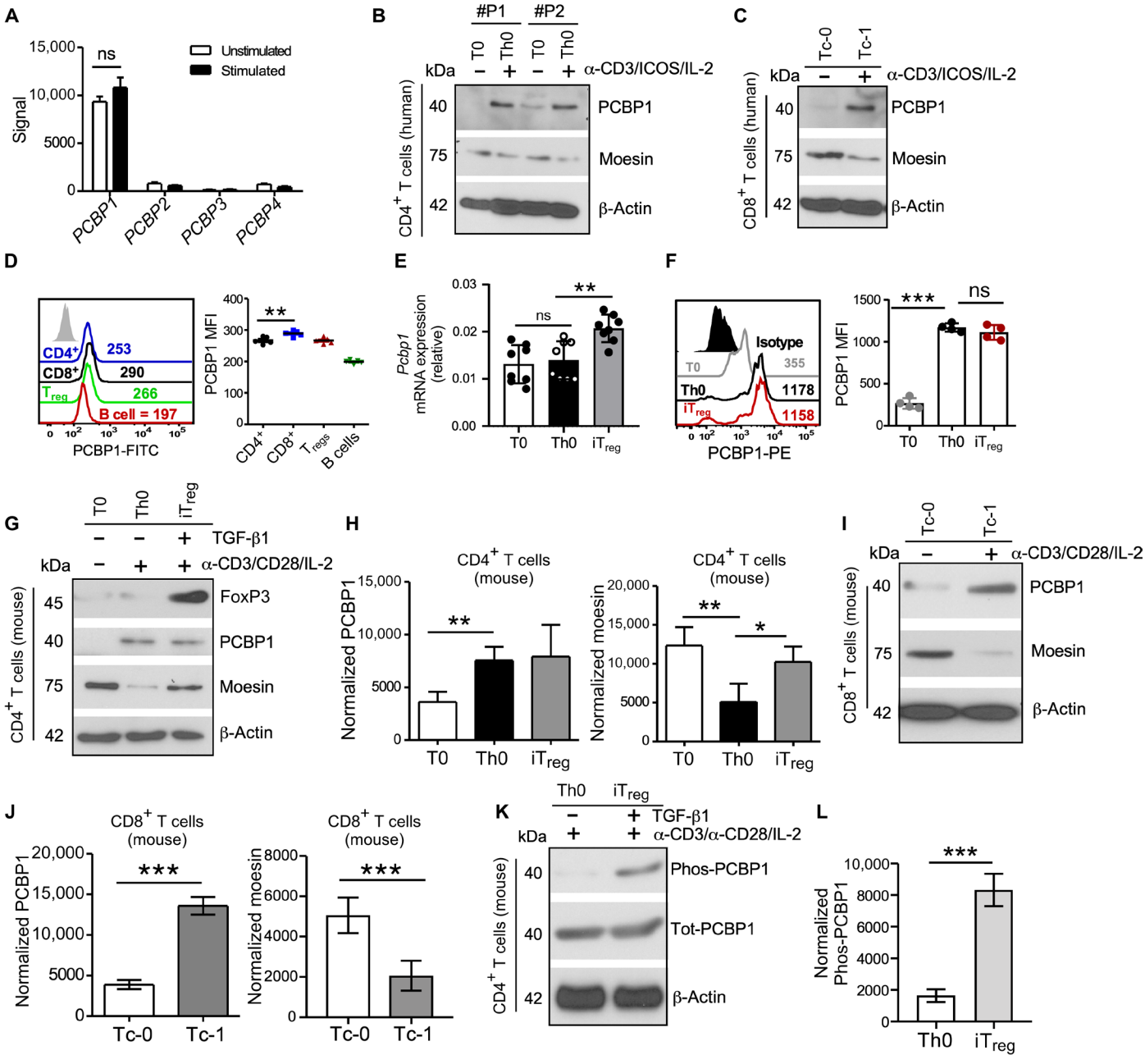

Fig. 1. Activated T cells up-regulate PCBP1. (**A**) Expression of mRNA encoding PCBP1-4 in human $CD3^+$ T cells before (Unstimulated) and after (Stimulated) stimulation for 24 hours with anti-CD3 and anti-CD28 (obtained from Gene Expression Omnibus accession code GSE13887). $n = 4$ biologically independent samples. (**B** and **C**) Immunoblotting for total PCBP1 and moesin expression in human $CD4^+$ (B) and $CD8^+$ (C) T cells left unstimulated (T0 and Tc-0) or stimulated (Th0 and Tc-1) with antibodies against CD3 and ICOS with IL-2 for 4 days. β-Actin was used as loading control. (**D**) Flow cytometry (left) and quantification (right) of PCBP1 expression in subsets of splenic lymphocytes from mice. FITC, fluorescein isothiocyanate. (**E** and **F**) Relative *Pcbp1* mRNA expression (E) and fluorescence-activated cell sorting (FACS) analysis and PCBP1 mean fluorescence intensity (MFI) in subsets of in vitro polarized T cells. (E) $n = 8$; (F) $n = 4$. PE, phycoerythrin. (**G** and **H**) Immunoblotting of moesin, PCBP1, FoxP3, and β-actin (G) and quantification for PCBP1 and moesin (H) using splenic mouse $CD4^+$ T cells activated with anti-CD3 and anti-CD28 for 3 days in the absence (Th0) or presence (iT_{reg}) of TGF-β in vitro. $n = 5$. (**I** and **J**) Mouse splenic $CD8^+$ T cells from the same experiments as (G and H). $n = 5$. (**K** and **L**) Immunoblotting for phosphorylated and total PCBP1 (K) in Th0 and iT_{regs} and quantification (L). (D) Error bars represent means ± SE and (E, F, H, J, and L) SD; $^*P < 0.05$, $^{**}P < 0.01$, and $^{***}P < 0.001$ (Student's *t* test); ns, not significant.

of the X chromosome in these mice, the T_{reg} cell compartment contains a mix of PCBP1-sufficient *Foxp3-YFP*$^-$ and PCBP1-deficient *Foxp3-YFP*$^+$ cells. PCBP1 mixed chimeric WT mice are heterozygous for *Foxp3*$^{YFP\text{-}Cre}$ and contain WT *Pcbp1* gene. PCBP1 chimeric KO T_{regs} showed no major changes in multiple T_{reg} signature molecules, except for CTLA-4 and PD-1, which were decreased and increased, respectively, in the chimeric KO T_{regs} (Fig. 2I and fig. S4B).

These results indicate that PCBP1 has a fundamental role in subverting T_{reg} phenotype in undifferentiated T cells. That is, deletion of PCBP1 in early thymocytes using the *Cd4*-Cre system shifts

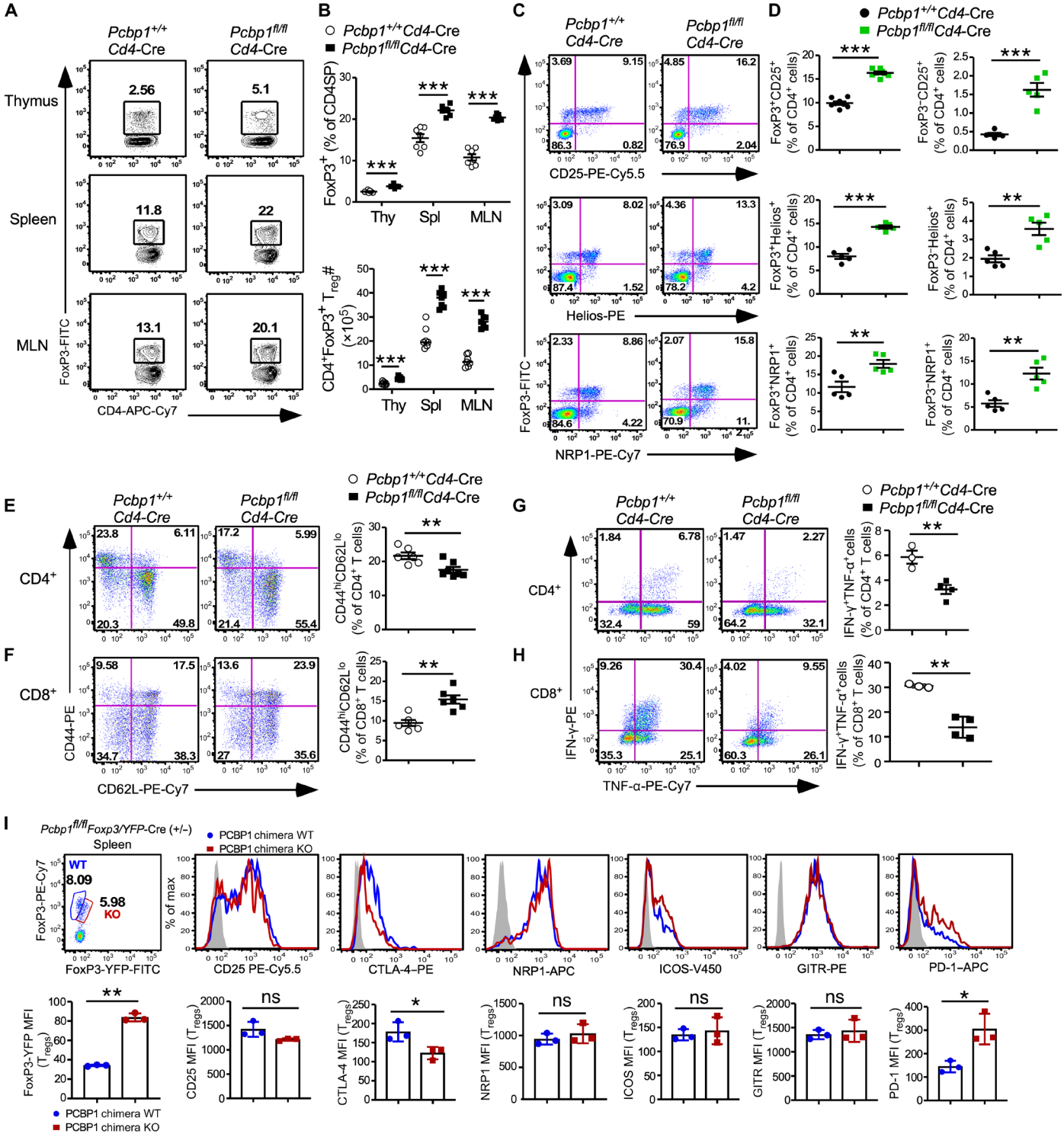

Fig. 2. Loss of PCBP1 causes optimal T_{reg} cell development but is not required for the maintenance of T_{regs}. (**A** and **B**) Intracellular FoxP3 in $CD4^+CD8^-$ thymocytes (Thy) and peripheral T cells from the spleen (Spl) and mesenteric lymph nodes (MLN) (A) and quantification (B). $n = 7$. (**C** and **D**) Frequencies of CD25-, Helios-, and NRP1-expressing T cells among $CD4^+FoxP3^+$ T_{regs} (C) and $CD4^+FoxP3^-$ T cells (D) from the spleen of *Pcbp1*$^{+/+}$*Cd4*-Cre and *Pcbp1*$^{fl/fl}$*Cd4*-Cre mice. $n = 5$. (**E** and **F**) Representative flow cytometry plots of CD44 and CD62L (left) and quantification (right) in splenic $CD4^+$ (E) and $CD8^+$ (F) T cells from WT and *Pcbp1*$^{fl/fl}$*Cd4*-Cre mice ($n = 6$). (**G** and **H**) Percentage IFN-γ^+TNF-α^+–producing T cells (left) and quantification (right) of $CD4^+$ (G) and $CD8^+$ (H) T cells stimulated with phorbol 12-myristate-13-acetate (PMA)/ionomycin in the presence of brefeldin A for 2 hours (WT, $n = 3$; KO, $n = 4$). (**I**) Histograms of CD25, CTLA-4, NRP1, ICOS, GITR, and PD-1 MFI (top) and quantification (bottom) in splenic T_{regs} from *Pcbp1*$^{fl/fl}$*Foxp3*/YFP-Cre$^{+/-}$ chimera female mice. $n = 3$. (B to I) Error bars represent means ± SE. $^*P < 0.05$, $^{**}P < 0.01$, and $^{***}P < 0.001$ (Student's *t* test).

conventional T cells (T_{convs}) to the T_{reg} lineage and confer increased T_{reg} hallmark molecules (figs. S2, D and E, and S3A). However, loss of PCBP1 after FoxP3 expression in matured T_{regs} using the *Foxp3*-YFP-Cre system does not cause major changes (Fig. 2I and fig. S4, A and B). This dichotomy underscores the importance of phosphorylated PCBP1, which contributes to the RNA binding activity and function of the protein. WT quiescent T_{convs} have reduced TGF-β signaling (*29*), so PCBP1 is unphosphorylated and retains its RNA binding activity, thus preventing the expression of T_{reg} commitment genes by effector T cells upon activation. Deletion of PCBP1 using the *Cd4*-Cre system abolishes this repressive function, enables the expression of T_{reg} commitment mRNAs, promotes TGF-β signaling via increased moesin expression (*21*), and shifts T_{convs} toward a stable T_{reg} cell lineage (Fig. 2, A and B, and figs. S1G and S4C). In contrast, PCBP1 WT T_{regs} is phosphorylated because of higher TGF-β signaling (*18*, *30*, *31*), and its target mRNAs are derepressed to facilitate efficient T_{reg} cell differentiation (*21*). Thus, PCBP1 deletion in T_{regs} caused no major changes since T_{reg} commitment mRNAs were already liberated from PCBP1 control (figs. S1, F and G, and S4D). However, other mechanisms of PCBP1 function may also be involved.

PCBP1 endows effector T cell functions

We examined the possibility that PCBP1-deficient T cells are more poised to convert to T_{regs} in the right milieu. To examine this possibility, we used the aGVHD model to assess the effects of PCBP1 deletion on the generation of peripheral T_{regs}, as well as examine the ability of the developed T_{regs} to attenuate effector T cell responses. We hypothesized that PCBP1-WT naïve T cells transferred into mismatched recipient mice would be activated into effector T cells and drive the pathogenesis of aGVHD (*32*). In contrast, transfer of T cells lacking PCBP1, which appear poised to convert to T_{regs}, would shift into this suppressive lineage and confer resistance against aGVHD (*33*, *34*). To this end, T cell–depleted (TCD) bone marrow (BM) cells isolated from B6.CD45.1 mice were cotransferred intravenously with T_{reg}-depleted naïve $CD4^+$ and $CD8^+$ T cells (B6.CD45.2) and isolated from the spleen of WT and *Pcbp1*$^{fl/fl}$*Cd4*-Cre mice into irradiated BALB/c mice (Fig. 3A). Changes in body weight, clinical disease manifestation, and survival were monitored for up to 80 days after BM transplant (BMT), as reported previously (*35*). Some BALB/c recipient mice were transplanted with BM lacking only T cells. All recipient mice dropped body weight 2 days after BMT because of the irradiation but quickly recovered. As expected, mice that received only BM cells did not lose body weight nor did they display any clinical signs of aGVHD and remained healthy throughout the experiment (Fig. 3, B to D).

In contrast, recipients of PCBP1-sufficient T cells showed severe symptoms of aGVHD including rapid body weight loss and hair loss and consequently succumbed to the disease within 50 days after BMT (Fig. 3, B to D). However, the mice infused with PCBP1-deficient T cells displayed less body weight loss with minor clinical signs of aGVHD. Greater than 50% of the mice that received PCBP1-deficient T cells did not develop severe aGVHD and survived beyond 80 days after BMT (Fig. 3, B to D). These data suggest a critical requirement for PCBP1 in driving effector T cell function and pathogenicity.

To understand the relevant mechanisms for pathogenicity, we examined T cell functions based on the production of IFN-γ and TNF-α as the key mediators of aGVHD (*36*, *37*) in the spleen (lymphoid organ) and liver (GVHD target organ) on day 14 after BMT. There was significant reduction of IFN-γ and TNF-α by splenic PCBP1-deficient T cells compared to WT T cells but no difference in Tbet expression (Fig. 3E and fig. S5A). Notably, the proportion and number of $FoxP3^+$ T_{regs} among splenic $CD4^+$ and $CD8^+$ T cells in KO recipients was markedly increased (Fig. 3, F and G). Similar reduction in IFN-γ and TNF-α and conversion to T_{regs} by PCBP1-deficient $CD4^+$ and $CD8^+$ T cells were also observed in the liver (Fig. 3, H to J, and fig. S5B).

In another experiment, we determined the function of lentiviral short hairpin RNA (shRNA) *Pcbp1* knockdown (KD) $CD4^+CD25^-$ T cells in a model of type 1 diabetes. Nonobese diabetic (NOD) *Rag1*$^{-/-}$ recipient mice were infused with WT iT_{regs} or with activated T cells (Th0) transduced with scrambled virus or shRNA targeting *Pcbp1*. Whereas mice infused with scrambled Th0 cells succumbed to hyperglycemia by week 5, *Pcbp1* KD Th0 cells significantly delayed the onset of type 1 diabetes in recipient mice, similar to mice infused with WT iT_{regs} (Fig. 3, K and L). These findings are consistent with our observations that T cells lacking PCBP1 shift toward $FoxP3^+$ T_{regs} in response to TCR signaling. The generated T_{regs} from T cells lacking PCBP1 maintain immunosuppressive functions by conferring protection against aGVHD and type 1 diabetes. Together, our data indicate that PCBP1 distinctively regulates effector versus T_{reg} cell differentiation to shape tolerance and immunity.

PCBP1 prevents expression of T_{reg} signatures in effector T cells

To investigate the mechanism for enhanced generation of T_{regs} in the PCBP1-deficient mice, we performed RNA sequencing (RNA-seq). Total RNA was extracted from splenic $CD4^+$ T cells of 6-to 8-week-old *Pcbp1*$^{fl/fl}$*Cd4*-Cre and WT littermates. Initial analyses confirmed the quality of the data output (fig. S6, A and B). We next predicted the biological functions of the differentially expressed genes (DEGs) using the ToppGene Suite. We observed extensive alterations in gene expression due to loss of PCBP1 in T cells, and the most significant enrichment of the DEGs was related to T_{reg} cell pathways (Fig. 4, A and B). We found that the enriched Gene Ontology (GO) terms for DEGs were related to the cell cycle and immune system including T cell activation and differentiation, as well as antigen processing and presentation (Fig. 4C). Consistent with the impaired proliferation of T cells and decreased cell numbers observed in PCBP1-deficient mice (fig. S2), we found dysregulation of numerous cell cycle– and apoptosis-related pathways and genes (Fig. 4C and fig. S6C).

In addition to the cell cycle–related genes, there was enrichment of several DEGs [false discovery rate (FDR) < 0.05] that play important roles in T_{reg} cell development, stability, and suppressive function. Examples include *Foxp3*, *Klrg1*, *Nrp1*, *Nrp2*, *Ahr*, *Myb*, *Il2ra* (CD25), *Entpd1* (which encodes CD39), *Gzmb*, *Tgfb1*, and *Bmp1* in $CD4^+$ T cells lacking PCBP1 (Fig. 4, B to D, and fig. S6C) (*38*, *39*). In contrast, but consistent with our observations, genes essential for effector T cell activation and function such as *Lck*, *Cd28*, *Zap70*, and *Tcf7* were significantly decreased (FDR < 0.05) in $CD4^+$ T cells lacking PCBP1 expression (Fig. 4D and fig. S6C). In agreement with data from our GVHD experiments, we also found cytokine genes such as *Ifng*, *Tnf*, *Il21*, and *Csf2* (which encodes GM-CSF) to be significantly less in $CD4^+$ T cells lacking PCBP1 compared to controls (Fig. 4, C and D). Thus, in the absence of PCBP1, $CD4^+$ T cells expressed less of cytokine genes important for effector T cell functions but enhanced expression of T_{reg} signature genes such as *Foxp3*, *Il2ra*, *Klrg1*, and *Nrp1*. These results indicate

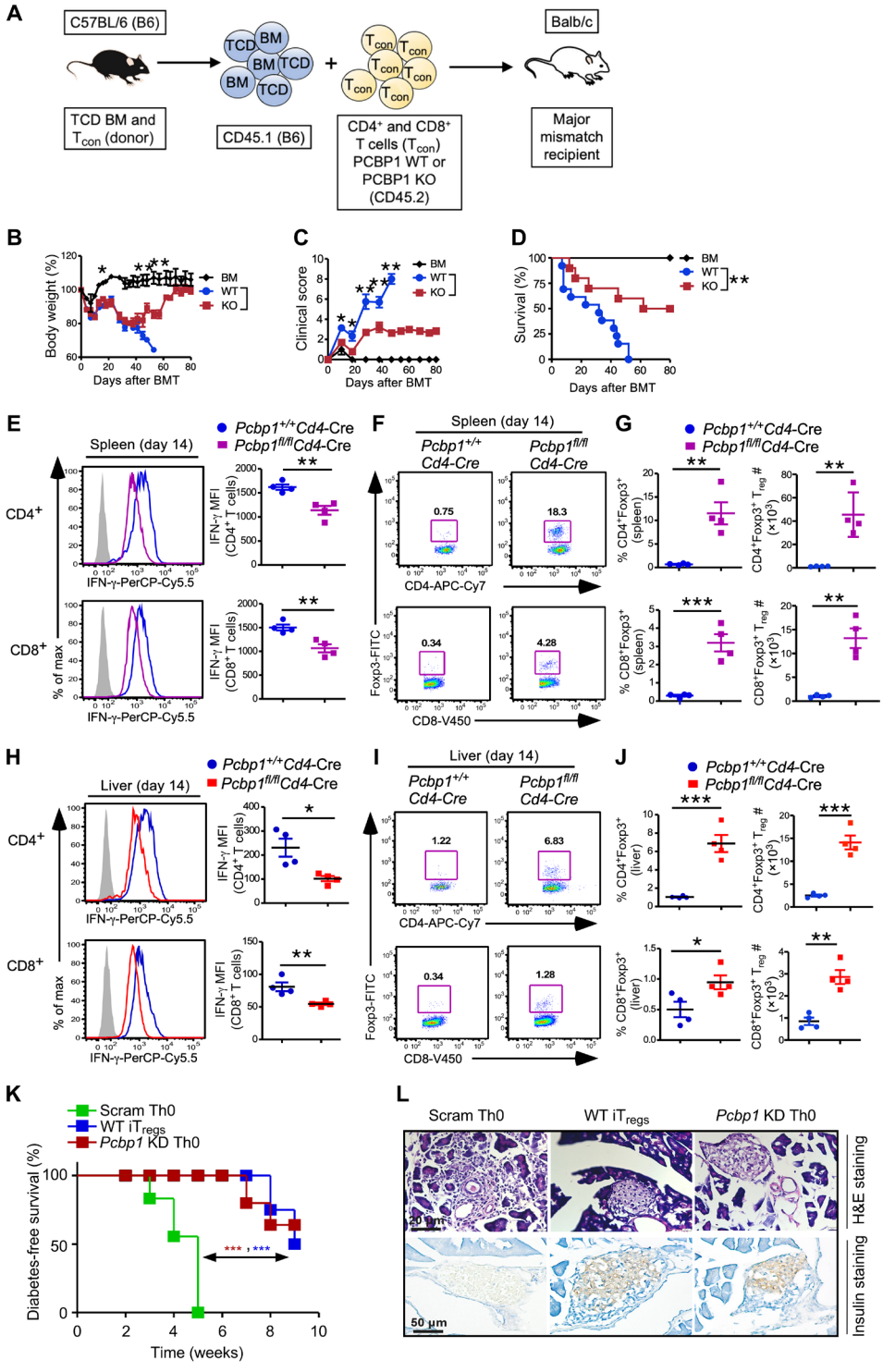

Fig. 3. PCBP1 is essential to drive optimal effector T cell functions but limits T_{reg} cell differentiation. (**A** to **D**) Purified CD25-depleted PCBP1 WT or PCBP1 KO donor T cells (7×10^5; H-2^b) were transferred into lethally irradiated (700 centigray) BALB/c (H-2^d) mice transplanted with 5×10^6 TCD BM cells per mouse. Schematic for aGVHD using PCBP1 WT and KO T cells (A), average body weight of the GVHD mice (B), clinical scores (C), and survival (D) of recipient mice monitored as indicated. (**E**) FACS analysis and percentage of IFN-γ MFI in $CD4^+$ and $CD8^+$ T cells from spleen cells stimulated with PMA/ionomycin for 4 hours from GVHD mice on day 14 after allo-BMT. (**F** and **G**) Frequency of $FoxP3^+$ T_{regs} (F) and quantification (G) on day 14 after allo-BMT in the spleen of WT and PCBP1 KO T cell recipients. (**H**) Expression of IFN-γ (left) and quantified plots (right) in the liver day 14 after allo-BMT. (**I** and **J**) $FoxP3^+$ T_{regs} (I) and quantification (J) in the liver of recipient mice on day 14. (**K** and **L**) Diabetes-free survival and histology in diabetes model following transfer of scrambled or Pcbp1 knockdown (KD) or WT iT_{regs}. Diabetes-free survival curve (I), and hematoxylin and eosin (H&E; top)– and insulin (bottom)–stained pancreatic sections from recipient mice (J). (B, C, E, G, H, and J) Error bars represent means ± SE. *$P < 0.05$, **$P < 0.01$, and ***$P < 0.001$ (Student's *t* test); (D and K) by log-rank (Mantel-Cox) test.

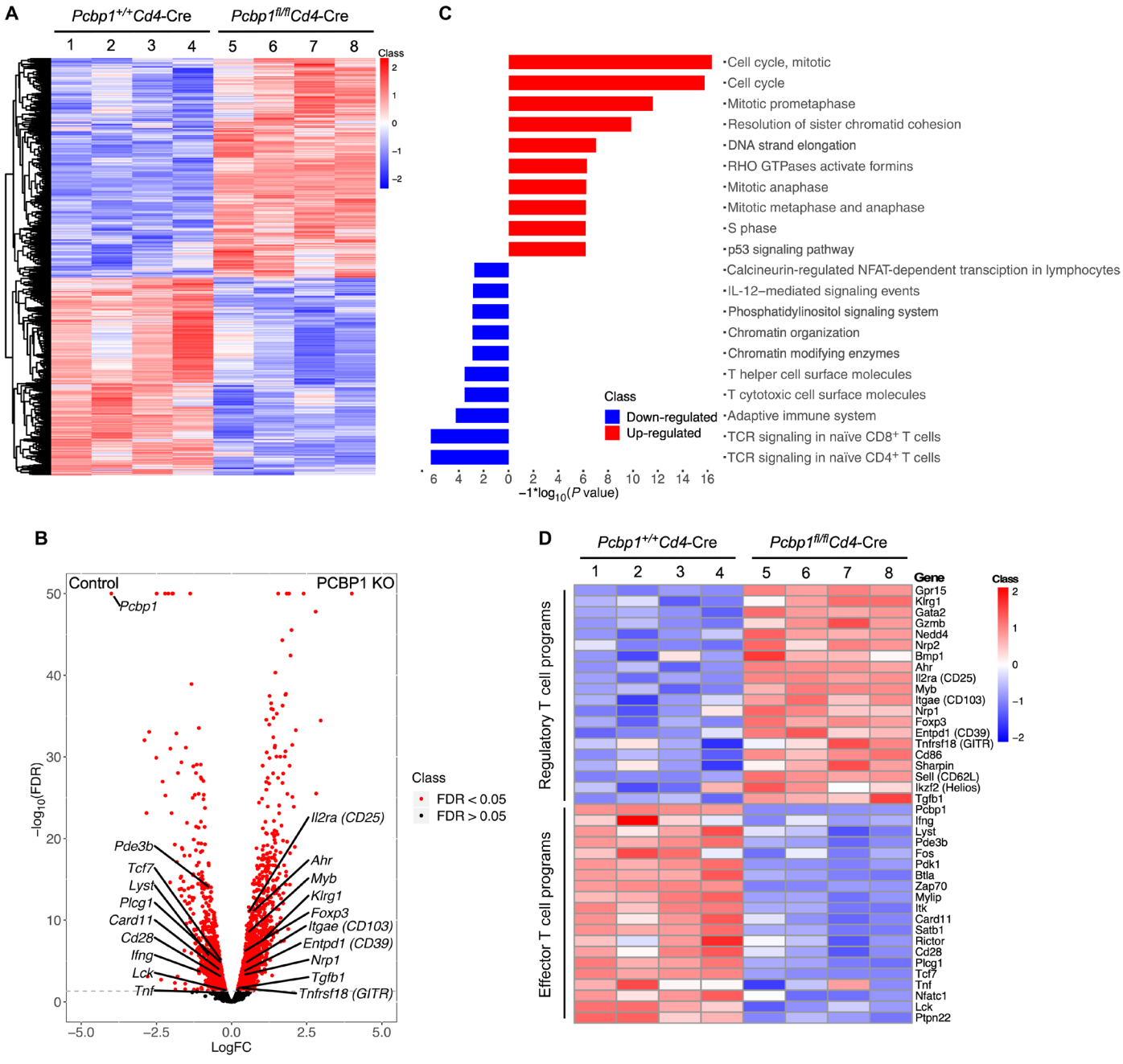

Fig. 4. Effector T cell–intrinsic T_{reg} commitment programs are constrained by PCBP1. (**A**) Heat map of DEGs (FDR < 0.1 and absolute $\log_2$ fold change > 0.2) in $CD4^+$ cells isolated from the spleen of 6-week-old *Pcbp1*$^{+/+}$*Cd4*-Cre ($n = 4$) and *Pcbp1*$^{fl/fl}$*Cd4*-Cre ($n = 4$) mice. (**B**) Volcano plot showing differential gene expression in mice. (**C**) Enrichment of DEGs (FDR < 0.05) in mice for biological process GO terms. GTPases, guanosine triphosphatases. (**D**) Heat map of up-regulated T_{reg} cell signature and down-regulated effector T cell signature genes (FDR < 0.05) in *Pcbp1*$^{+/+}$*Cd4*-Cre ($n = 4$) and *Pcbp1*$^{fl/fl}$*Cd4*-Cre ($n = 4$) mice.

that PCBP1 plays a pivotal role in controlling the expression of effector T cell–intrinsic T_{reg} transcriptional signatures to shape effector versus T_{regs}. An intriguing concept is that PCBP1 functions as a global intracellular immune checkpoint against T_{reg} cell programs; thus, targeting it may modulate antitumor responses. It also suggests that PCBP1 expression may be necessary to stabilize and sustain the function of effector T cells in cancer.

PCBP1 constrains optimal TGF-β signaling and iT_{reg} differentiation in vitro

To further ascertain that PCBP1 inhibits the conversion of activated T cells to T_{regs} and, thus, T cells lacking PCBP1 are poised to differentiate to T_{regs}, we first knocked down *Pcbp1* in splenic $CD4^+CD25^-$ T cells using a lentiviral shRNA system and cultured under iT_{reg} differentiating conditions with anti-CD3/anti-CD28 antibodies and

IL-2, in the presence or absence of TGF-β (5 ng/ml) for 3 to 5 days. KD efficiency and liberation of the PCBP1 targets moesin and eiF5A2 (*20*, *40*) were confirmed by immunoblotting (Fig. 5A and fig. S7A). We next assessed the frequency of FoxP3$^+$ iT$_{regs}$ and found that more *Pcbp1* KD T cells were converted to iT$_{regs}$ compared to scrambled, even without the addition of exogenous TGF-β (Fig. 5, B and C).

Next, we cocultured naïve CD4$^+$CD25$^-$ T cells isolated from the spleen of *Pcbp1*$^{fl/fl}$*Cd4*-Cre mice or littermate controls in vitro with IL-2 and allogenic dendritic cells (DCs) isolated from BALB/c mice in the presence or absence of TGF-β1. We found that PCBP1-deficient CD4$^+$CD25$^-$ T cells differentiated more robustly to mature FoxP3$^+$CD25$^+$ T$_{regs}$ after 5 days compared to PCBP1-sufficient T cells (Fig. 5, D and E). PCBP1-deficient CD4$^+$CD25$^-$ T cells cocultured with DCs in the absence of TGF-β1 also appeared more poised to differentiate into T$_{regs}$ than WT CD4$^+$CD25$^-$ T cells on the basis of the greater frequency of FoxP3$^-$CD25$^+$ pre-T$_{regs}$ (Fig. 5E). These results further suggested that PCBP1 inhibits differentiation to FoxP3$^+$ T$_{regs}$; thus, its deletion confers increased conversion of activated T cells to the T$_{reg}$ cell lineage. Further examination also showed increased phosphorylated Smad2/3 levels in *Pcbp1* KD T cells (Fig. 5F and fig. S7B), which was corroborated by increased expression of the TGF-β–docking receptor GARP (Glycoprotein A repetitions predominant) (Fig. 5G) (*41*). Together, these data suggested that PCBP1 plays important roles in preventing activated T cells from differentiating into T$_{regs}$ via inhibition of pertinent T$_{reg}$ signaling pathways such as TGF-β signaling.

Loss of PCBP1 in T cells blunts antitumor responses

To test the role of PCBP1 during antitumor responses, we compared the growth of MC38 colon cancer cells in WT mice versus mice lacking PCBP1 in T cells. We observed exponential MC38 tumor growth in both WT and *Pcbp1*$^{fl/fl}$*Cd4*-Cre mice (Fig. 6A); however, tumor size and weight were significantly greater in *Pcbp1*$^{fl/fl}$*Cd4*-Cre mice (Fig. 6, A and B). In further agreement with the increased TGF-β signaling under reduced PCBP1 conditions (Fig. 5, F and G) and previous reports that demonstrated that PCBP1 loss promotes tumor metastasis (*18*), we also observed an enlarged spleen in tumor-bearing PCBP1 KO mice compared to WT littermates (Fig. 6C). Flow cytometry analysis showed increased percentage of CD45$^-$ tumor cells in the spleen of *Pcbp1*$^{fl/fl}$*Cd4*-Cre mice (Fig. 6D). Consistently, WT CD8$^+$ and CD4$^+$ tumor-infiltrating lymphocytes (TILs) expressed higher PCBP1 compared to splenic T cells (Fig. 6E). Absolute numbers of CD4$^+$ and CD8$^+$ T cell populations were decreased in the tumor-draining lymph nodes (TDLNs) between WT and *Pcbp1*$^{fl/fl}$*Cd4*-Cre mice. Moreover, the frequency and numbers of CD4$^+$ and CD8$^+$ T cells were significantly less in the tumors of *Pcbp1*$^{fl/fl}$*Cd4*-Cre mice compared to WT (Fig. 6, F and G), suggesting that PCBP1 is crucial for antitumor T cells to proliferate effectively and infiltrate tumors.

We then analyzed FoxP3 expression in CD4$^+$ T cells and found that it increased in the spleen of *Pcbp1*$^{fl/fl}$*Cd4*-Cre mice but was similar in the tumors and unchanged in CD8$^+$ T cells (fig. S8, A and B). Furthermore, IFN-γ– and TNF-α–producing T cells were significantly impaired in *Pcbp1*$^{fl/fl}$*Cd4*-Cre mice (Fig. 6, H and I). These data suggested that PCBP1 is up-regulated in tumor-infiltrating T cells to support ongoing antitumor immune responses. However, T cell–specific loss of PCBP1 in the tumor microenvironment due, in part, to increased TGF-β signaling blunts antitumor immunity and promotes tumor progression and metastasis.

Loss of PCBP1 promotes immune suppression and is a potential predictor of response to ICB

The breakdown in the function of PCBP1-deficient T cells, compared to WT, prompted us to investigate whether PCBP1 loss creates an immune-suppressive tumor microenvironment that supports tumor progression. ICB has revolutionized cancer treatment, but further improvements are still required to better predict patients more likely to benefit from this treatment. We analyzed tumor CD8$^+$ and CD4$^+$ non-T$_{regs}$ from WT and *Pcbp1*$^{fl/fl}$*Cd4*-Cre mice for expression of inhibitory immune checkpoint receptors and the T$_{reg}$ suppressive molecule CD73. We found a clear increase in PD-1, TIGIT (T Cell Immunoreceptor with Ig and ITIM Domains), VISTA (V-domain Ig suppressor of T cell activation), and CD73, but not CTLA-4, on CD8$^+$ T cells from *Pcbp1*$^{fl/fl}$*Cd4*-Cre mice compared to WT littermates (Fig. 7A). In addition, TIGIT and VISTA on CD8$^+$ T cells in the TDLN were unchanged or decreased, respectively, in *Pcbp1*$^{fl/fl}$*Cd4*-Cre mice. Unlike tumor-infiltrating CD8$^+$ T cells, CD8$^+$ T cells from the TDLN of *Pcbp1*$^{fl/fl}$*Cd4*-Cre mice displayed higher CD73 expression compared to WT cells (fig. S8C). PD-1 and CTLA-4 were higher on CD4$^+$FoxP3$^+$ T$_{regs}$ from the spleen and tumor of PCBP1 KO mice (fig. S8, D and E).

In another experiment, WT and *Pcbp1*$^{fl/fl}$*Cd4*-Cre mice were challenged with MB49 bladder cancer cells. Again, tumor growth was more rapid in PCBP1-deficient mice compared to WT animals (fig. S8F). Consistently, the spleen of KO mice was enlarged with a greater frequency of CD45$^-$ cells compared to WT mice (fig. S8, G to I). We detected increased proportions of FoxP3$^+$CD25$^-$ cells among CD4$^+$ T cells in the tumors of PCBP1 KO mice (fig. S8, J and K), suggesting that loss of PCBP1 helps expand or maintain this immature T$_{reg}$ subset (*42*). Similar to the MC38 model and in line with PCBP1 loss promoting immunosuppression, we detected increased PD-1 expression on TILs from *Pcbp1*$^{fl/fl}$*Cd4*-Cre mice relative to WT littermates (fig. S8, L and M). Together with our RNA-seq data, the increase of inhibitory checkpoint receptors PD-1, TIGIT, and VISTA, as well as the reduced functionality (Figs. 6, H and I, and 7, A and B) in PCBP1-deficient T cells, is indicative of immune exhaustion under reduced PCBP1 conditions. We hypothesized that in such an immune-suppressive setting, ICB would be more effective; thus, PCBP1 could potentially serve as a predictor of response to immunotherapy.

We took advantage of the published RNA-seq database currently available from studies on patients with melanoma before and after anti–PD-1 antibody treatment and examined *PCBP1* gene expression. Data from Hugo *et al.* (*43*) provide a comprehensive analysis of combined RNA-seq results obtained from melanoma patients. We found that complete responders to PD-1 blockade also had the lowest *PCBP1* expression compared to partial or progressive responders (Fig. 7C). Patients with the lowest *PCBP1* expression before treatment (Q1 and Q2) responded better to ICB and survived longer compared to melanoma patients with higher PCBP1 (Q3 and Q4) (Fig. 7D). These findings suggest a dichotomy between *PCBP1* expression and responsiveness to ICB in cancer. In a nontumor setting, higher PCBP1 stabilizes effector T cell functions to generate immune responses that obstruct tumorigenesis. In cancer, higher PCBP1 levels counteract immune exhaustion by preventing the expression of factors such as moesin, PD-1, and TGF-β signaling that promote immunosuppression. ICB would be less effective under such conditions. In contrast, lower PCBP1 or phosphorylation of PCBP1 elicited by TGF-β liberates expression of multiple factors that drive an immune-suppressive tumor microenvironment. This setting is more

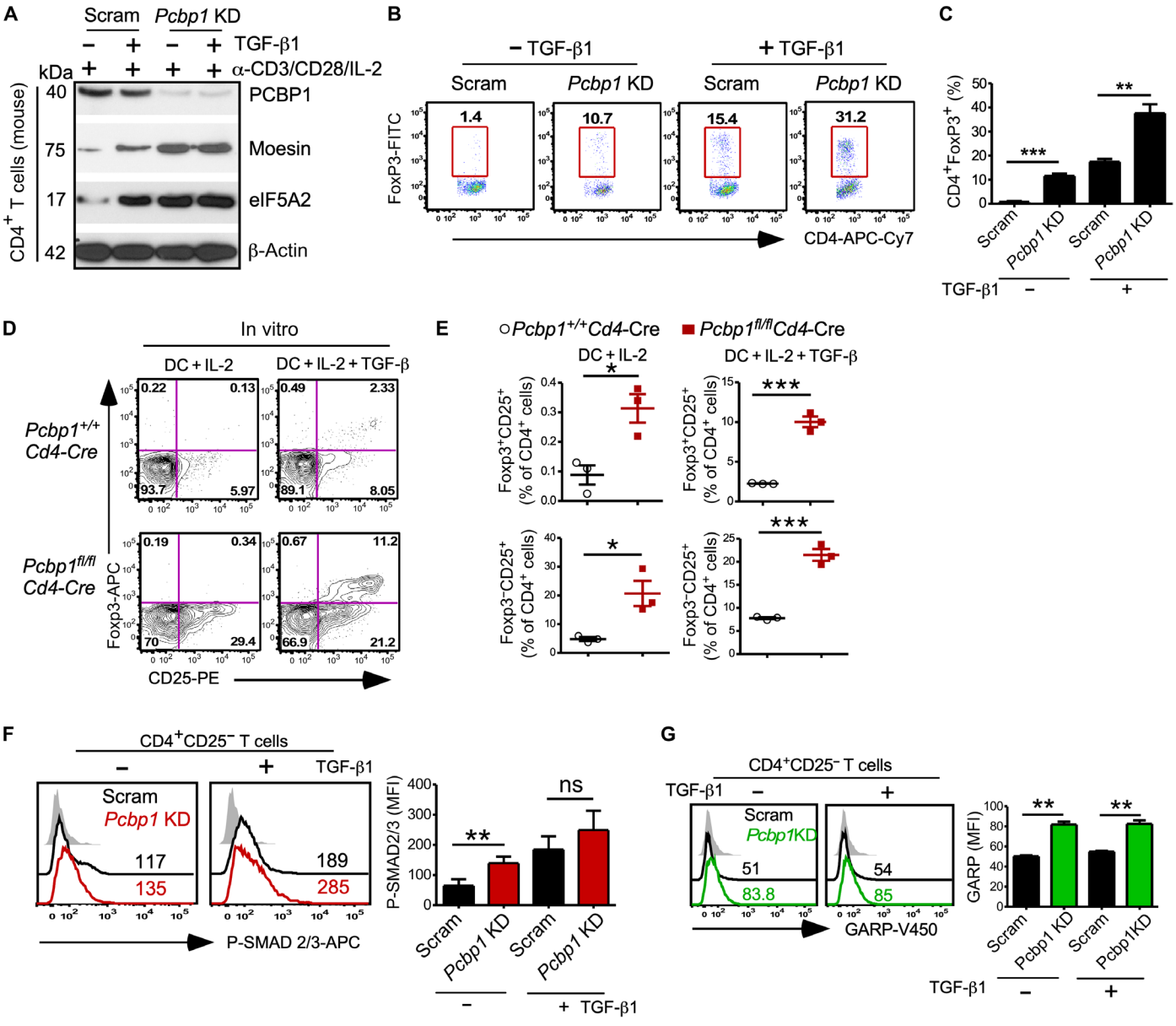

Fig. 5. Increased frequency of FoxP3$^+$ T_{regs} and enhanced TGF-β signaling in T cells expressing lower PCBP1. Splenic CD4$^+$CD25$^-$ T cells were transduced with scrambled (Scram) or lentiviral shRNA targeting *Pcbp1* for 48 hours and cultured in the absence or presence of exogenous TGF-β under iT_{reg} conditions. (**A**) Immunoblotting of PCBP1 and targets moesin and eIF5A2. β-Actin is shown as loading control. (**B** and **C**) FACS analysis (B) and quantification (C) of FoxP3$^+$ T cells 5 days after lentiviral transduction. (**D** and **E**) Flow cytometry analyzing CD25-expressing cells among FoxP3$^+$ and FoxP3$^-$ T cells (D) and quantification (E) after in vitro culture of splenic CD4$^+$CD25$^-$ T cells from *Pcbp1*$^{f/f}$ and *Pcbp1*$^{f/f}$*Cd4*-Cre littermates with allo-DCs in the presence of IL-2 and with or without exogenous TGF-β1 (5 ng/ml). $n = 3$. (**F**) Flow cytometry of phospho-Smad2/3 and quantification. (**G**) Analysis of GARP expression and quantification in scrambled versus *Pcbp1* KD T cells. (C and E to G) Error bars represent means ± SD; $^*P < 0.05$, $^{**}P < 0.01$, and $^{***}P < 0.001$ (Student's *t* test).

conducive to ICB. These data further suggest that assessment of PCBP1 expression before checkpoint blockade therapy could be a potential predictor of response to ICB in patients.

DISCUSSION

The balance between T_{regs} and effector T cells, or tolerance and immune responses, respectively, is paramount to maintaining homeostasis and preventing the development of autoimmune and/or inflammatory diseases. While T_{regs} restrict immune function (*44*, *45*), effector T cells promote immune responses against infection and cancer (*46*, *47*). The fundamental roles of RBPs in the immune system have gained considerable attention in recent years because of their involvement in multiple immune processes and emerged as potential therapies (*48*, *49*). Of these RBPs, PCBP1 has mainly been studied in transformed epithelial cells for its role in cancer metastasis and progression (*50*, *51*). In addition, PCBP1 also exhibits iron chaperone activity toward ferritin (*11*). However, knowledge on

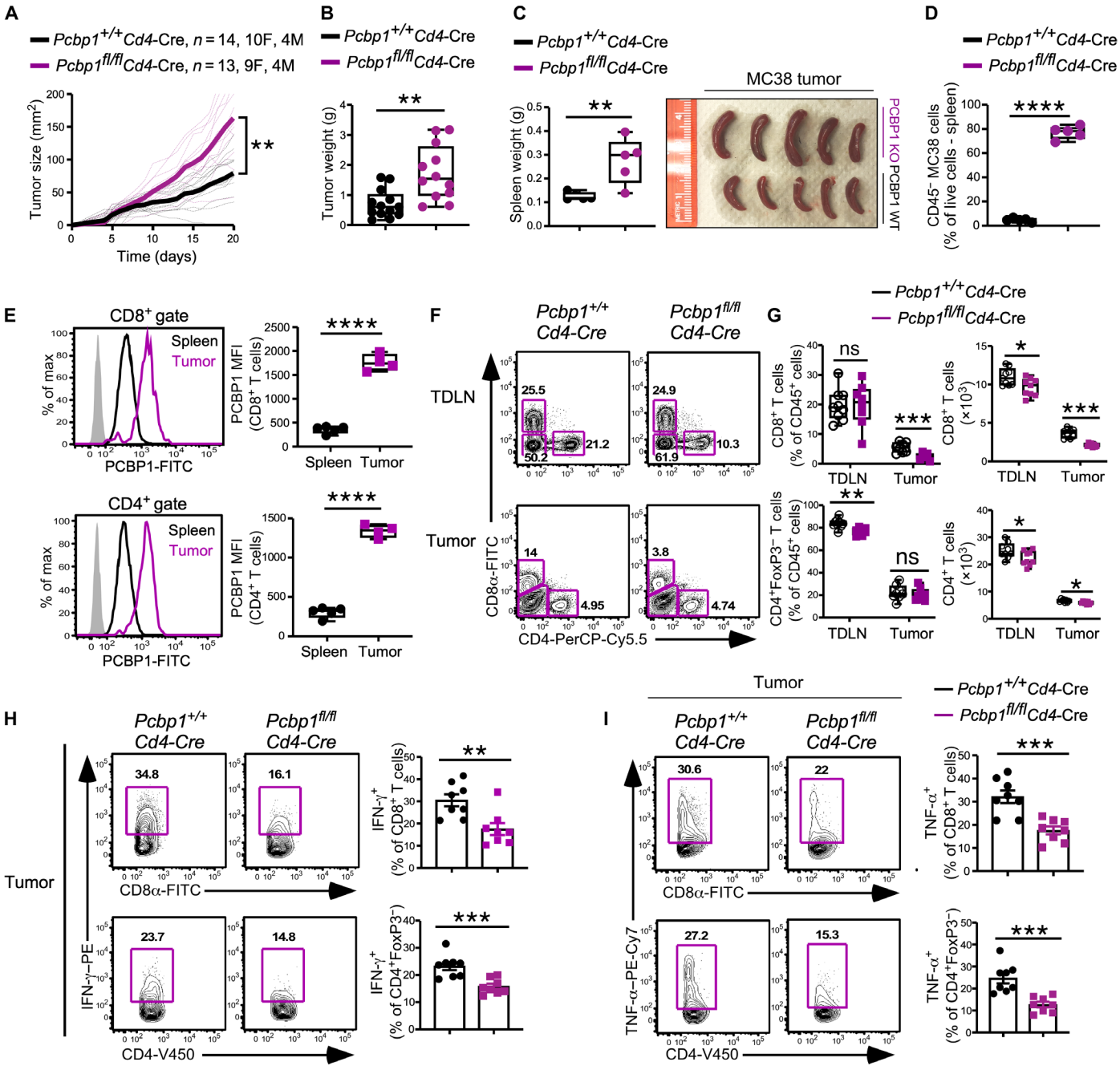

Fig. 6. Absence of PCBP1 in T cells compromise antitumor immunity. (**A**) Tumor growth over time following subcutaneous injection of MC38 cells (1×10^6) into *Pcbp1*$^{+/+}$*Cd4*-Cre ($n = 14$, 10 females and 4 males) and *Pcbp1*$^{fl/fl}$*Cd4*-Cre ($n = 13$, 9 females and 4 males) mice. (**B**) Tumor weight of *Pcbp1*$^{fl/fl}$*Cd4*-Cre ($n = 12$) and WT littermate ($n = 13$) mice as in (A). (**C**) Enlarged spleens measured (left) and representative examples (right). $n = 5$. Photo credit: E. A. Ansa-Addo, The Ohio State University. (**D**) Increased percentage of CD45$^-$ cells in the spleen of tumor-bearing *Pcbp1*$^{f/f}$*Cd4*-Cre compared with *Pcbp1*$^{f/f}$ littermates. $n = 5$. (**E**) Flow cytometry analysis of PCBP1 expression (left) and quantification (right) in CD8$^+$ (top) and CD4$^+$ (bottom) T cells from spleen and tumor of WT tumor-bearing mice. Spleen, $n = 5$; tumor, $n = 4$. (**F** and **G**) FACS analysis (F) and quantifications (G) of CD8$^+$ and CD4$^+$FoxP3$^-$ T cells among CD45$^+$ T cells from TDLN and tumor of WT and *Pcbp1*$^{fl/fl}$*Cd4*-Cre mice. TDLN, $n = 9$; tumor, $n = 8$. (**H**) Frequency of IFN-γ–producing cells among CD8$^+$ and CD4$^+$FoxP3$^-$ T cells in tumors from *Pcbp1*$^{fl/fl}$*Cd4*-Cre and WT littermates. $n = 8$. (**I**) Frequency of TNF-α–producing cells (left) and quantification (right) among CD8$^+$ and CD4$^+$FoxP3$^-$ T cells in tumors from *Pcbp1*$^{fl/fl}$*Cd4*-Cre and WT littermates determined by flow cytometry. $n = 8$. (B to I) Error bars represent means ± SE. $^*P < 0.05$, $^{**}P < 0.01$, $^{***}P < 0.001$, and $^{****}P < 0.0001$ (Student's *t* test); (A) two-way ANOVA.

PCBP1 function in T cell biology, particularly during differentiation of T cell subsets and T cell–mediated immune responses, is limited.

We recently reported that translational repression by PCBP1 is operational in CD4$^+$ T cells, but how this contributes to T cell fate specification remains unclear. PCBP1 repressed the translation of moesin mRNA and is rescued by TGF-β–mediated phosphorylation of PCBP1, which inhibits its RNA binding function (*21*). We demonstrated that moesin, in turn, promotes optimal TGF-β signaling,

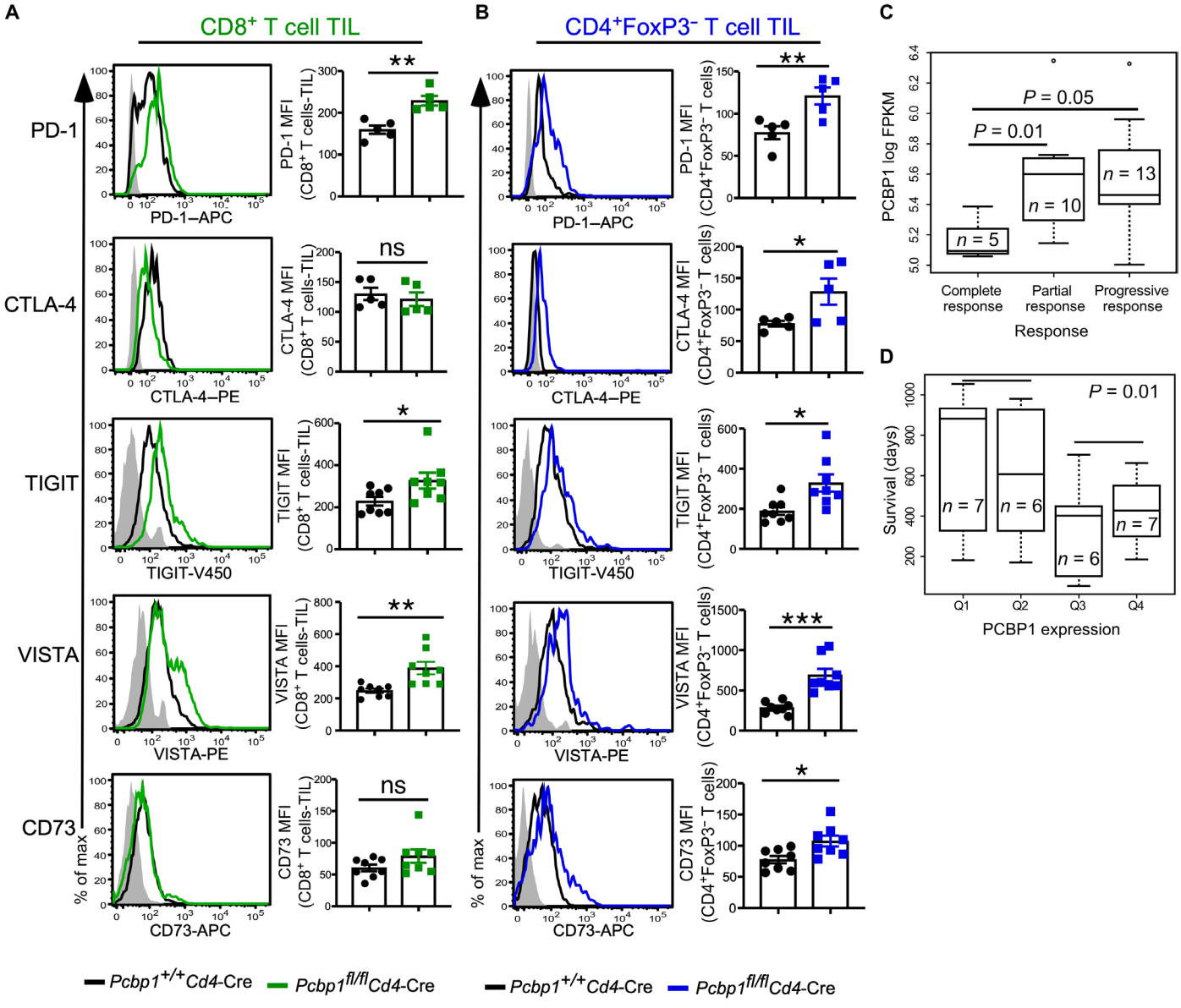

Fig. 7. Deletion of PCBP1 in T cells increases expression of checkpoint molecules and promotes immunosuppression. (**A** and **B**) Flow cytometric analysis (left) and quantification (right) of PD-1, CTLA-4, TIGIT, VISTA, and CD73 expression in tumor $CD8^+$ (A) and $CD4^+FoxP3^-$ (B) T cells from *Pcbp1*$^{+/+}$*Cd4*-Cre and *Pcbp1*$^{fl/fl}$*Cd4*-Cre. (**C**) Analysis of the clinical relevance of *PCBP1* mRNA according to response rate (separating complete responders, partial responders, and progressive responders). FPKM, fragments per kilobase of exon model per million reads mapped. (**D**) Significance of *PCBP1* mRNA expression (Q1, lowest; Q4, highest) and relationship to overall survival. (A and B) Error bars represent means ± SE. **P* < 0.05, ***P* < 0.01, and ****P* < 0.001 (Student's *t* test); (C and D) Mann-Whitney test.

which augments T_{reg} cell differentiation. Deletion of moesin potentiated adoptive T cell therapy and conferred protection against B16 melanoma in mice. In the present study, we have made several new discoveries that enhance our understanding about the roles of PCBP1 in T cell biology. We discovered that PCBP1 is up-regulated in both $CD4^+$ and $CD8^+$ T cells in response to activation. PCBP1 then restricts expression of T_{reg} signature molecules such as moesin in activated T cells to stabilize effector T cell functions.

We show that PCBP1 is an immune checkpoint required for effector T cell functions. PCBP1 is a global regulatory node that subverts immunosuppression in cancer. Because of the recent link between ICB and hyperprogression of cancer in some patients, it is paramount to accurately predict responders to immunotherapy (*7*). PCBP1 also contributes to efficient thymocyte development and peripheral T cell homeostasis. Mice with PCBP1-deficient T cells exhibited decreased matured thymocytes and peripheral T cells but increased pre-T_{regs}. We also found that the absence of PCBP1 resulted in increased T_{reg} cell conversion in the thymus and peripheral tissues. These data suggested that PCBP1 suppresses the expression of effector T cell–intrinsic T_{reg}-related molecules to maintain the identity of effector T cells. It also suggests that PCBP1 plays an active role as a negative immune checkpoint for excessive differentiation of $FoxP3^+$ T cells. We demonstrated using the aGVHD model that recipient mice transplanted with PCBP1-sufficient T cells

developed severe inflammation and succumbed to the disease. However, mice that received PCBP1-deficient T cells were remarkably protected. The GVHD model has been widely used to examine the functions of effector T cells and T_{regs} in either promoting or alleviating the pathogenesis of aGVHD, respectively (*52*).

Notably, PCBP1-deficient T cells robustly converted into peripheral T_{regs}, which produced less proinflammatory cytokines (IFN-γ and TNF-α) by day 14. However, PCBP1-sufficient T cells produced more cytokines and did not convert to peripheral T_{regs}. In another study, *Pcbp1* KD–activated T cells (Th0) delayed disease onset in a type 1 diabetes model. Further analysis confirmed our finding that absence of PCBP1 results in increased FoxP3$^+$ T_{regs} due, in part, to derepression of genes essential for commitment to the T_{reg} cell lineage. Previous studies have described mechanisms that constrain effector T cell functions to stabilize the development of T_{regs}. For example, the transcriptional repressors BACH2 and MiR-125a repress effector T cell programs to stabilize T_{reg}-mediated immune homeostasis (*53*, *54*). By contrast, the nuclear factor κB regulator A20 limits tT_{reg} development to promote effector functions (*55*). Thus, it is paramount to better characterize the molecular mechanisms that distinctively regulate the fate of effector cells versus T_{regs} in response to immune activation and against cancer.

By RNA-seq, we found that multiple T_{reg} signature or commitment genes were up-regulated in the absence of PCBP1. We also noted significant up-regulation of molecular pathways that impair T cell activation and proliferation such as *Tgfb1*, *Msn* (moesin), *Nrp1*, etc. Thus, mechanistically, our data suggest that PCBP1 is a global negative regulator of genes that promote the generation and stabilization of T_{regs}, as well as genes that support an immune-suppressive tumor microenvironment. Effector T cells intrinsically contain T_{reg} signature genes that, if expressed, would destabilize the effector lineage and cause them to switch into T_{regs}. PCBP1-deficient naïve T cells converted more efficiently to iT_{regs} in vitro compared to WT T cells from littermate mice. Our study also suggests that PCBP1 plays a nonredundant role in ensuring that T_{reg} commitment genes remain inhibited during acquisition of the effector T cell lineage. Such a global function in lymphocyte biology has been described for other RBPs (*56*, *57*).

Notably, PCBP1 is regulated by moesin via TGF-β signaling since moesin controls optimal TGF-β responses to maintain naïve T cell quiescence (*21*, *29*). Loss of PCBP1 in T cells exacerbated tumor growth in the MC38 colon cancer and MB49 bladder cancer models. Moreover, TILs lacking PCBP1 displayed signs of immune exhaustion by up-regulating several inhibitory immune checkpoint receptors and reduced antitumor cytokine production. By analyzing an RNA-seq dataset from a study by Hugo *et al.* (*43*), we found that patients with melanoma displaying lower PCBP1 responded better to anti–PD-1 therapy. Notably, this data also includes contributions from T cells and non–T cells. This dichotomy between *PCBP1* mRNA expression and response to ICB suggests PCBP1 as a potential predictor of response to immunotherapy and supports our conclusion that under reduced PCBP1 levels, factors that promote immune suppression such moesin, TGF-β signaling, and PD-1 are no longer restrained and therefore inhibit antitumor responses. Although there may be additional mechanisms involved, the results of our study implicate PCBP1 as a critical node for safeguarding effector T cell functions. It also suggests that PCBP1 limits excess differentiation of T_{regs} and constrains expression of inhibitory immune checkpoint molecules to impair immune exhaustion and immunosuppression. The potential role of RBPs as predictors of response to immunotherapy would offer great advancement to cancer treatment.

MATERIALS AND METHODS

Human peripheral blood mononuclear cells

Peripheral blood cells from healthy, deidentified individuals were purchased as a buffy coat (Plasma Consultants) or a leukophoresis (Research Blood Components). Lymphocyte enrichment was performed by centrifugation with Lymphocyte Separation Medium (Mediatech). Untouched CD4$^+$ and CD8$^+$ T cells were isolated by magnetic bead separation (Dynabeads, Thermo Fisher Scientific) and activated at a 1:5 bead–to–T cell ratio using magnetic beads (Dynabeads, Thermo Fisher Scientific) in complete T cell medium supplemented with recombinant human IL-2 (100 IU/ml; National Institutes of Health repository). T cells were harvested after 3 to 4 days, and lysates were prepared for immunoblotting. All procedures were performed under Institutional Review Board–approved protocols from the Medical University of South Carolina.

Mice

Pcbp1$^{f/f}$*Cd4*-Cre, *Pcbp1*$^{f/f}$*Foxp3*$^{YFP\text{-}Cre+}$, and *Pcbp1*$^{f/f}$*Foxp3*$^{YFP\text{-}Cre+/-}$ mice were generated in-house. *Pcbp1*$^{fl/fl}$, *Foxp3*$^{YFP\text{-}Cre}$, *Cd4*-Cre [Tg (Cd4-cre)1Cwi/BfluJ], and NOD*Rag1*$^{-/-}$, C57BL/6J have been described (*12*, *21*, *58*). Mice used for all experiments were on the C57BL/6 background, except for GVHD and diabetes model experiments. GVHD experiments were performed using BALB/c mice as donors for BM and were also used as recipients, and type 1 diabetes studies used NOD *Rag1*$^{-/-}$. In all studies comparing WT to PCBP1 KO mice, healthy, sex-matched, and age-matched littermates were used (male and female, 6 to 10 weeks of age unless stated otherwise). Notably, spleen and lymph nodes were kept separately throughout the study. Mice were housed in a specific pathogen–free barrier facility in ventilated cages with at most five animals per cage and provided with ad libitum food and water. With the exception of type 1 diabetes studies, which used NOD *Rag1*$^{-/-}$ immunodeficient mice, all studies used immune-competent mice that were treatment naïve until the start of study. No differences in phenotype were noted between WT and PCBP1 KO in T cells or T_{reg}-specific cells, and animals were genotyped for floxed alleles and CRE allele. All mouse procedures were performed under Institutional Animal Care and Utilization Committee–approved protocols from The Ohio State University and the Medical University of South Carolina (tumor, type 1 diabetes, and GVHD models) and conformed to all relevant regulatory standards.

Cell lines and in vitro cultures

Primary mouse T cell cultures from the spleen of male and female mice were used to set up T cell in vitro experiments in T cell media at 37°C with 5% CO_2 humidified conditions. T cell media contained RPMI 1640 media (catalog no. 10-40-CV) supplemented with 10% fetal bovine serum (FBS), 1% penicillin-streptomycin, Hepes, β-mercaptoethanol, sodium pyruvate, and nonessential amino acids. shRNA lentiviral particles were generated using human embryonic kidney (HEK) 293FT cell lines [American Type Culture Collection (ATCC)] cultured in Dulbecco's modified Eagle's medium (DMEM) (HyClone, USA). Tumor experiments were performed using MC38 colon cancer (ATCC) and MB49 bladder cancer cell lines (gift from S. Li, Harvard University, USA) all maintained in

DMEM, supplemented with 10% FBS heat-inactivated with penicillin-streptomycin.

T cell culture and differentiation in vitro

Briefly, $CD4^+$ T cells were isolated (catalog no. 130-104-454) from WT animal and *Pcbp1*$^{f/f}$*Cd4*-Cre mice and activated for 3 to 4 days via anti-CD3/anti-CD28 antibodies (5 μg/ml) plate bound (CD3, catalog no. 16-0031-85; CD28, catalog no. 16-0281-85). For differentiation experiments, naïve $CD4^+$ T cells from WT or KO animals were plated with α-CD3/CD28 antibodies (as above) and IL-2 in the presence of subset-specific cytokines and antibodies (iT_{reg}: TGF-β1, α–IFN-γ, and α–IL-4). In other experiments, allo-DCs were used instead of anti-CD28 antibody for polarization to iT_{regs}. Th0 experiments were performed under differentiation conditions (α-CD3/CD28 antibodies and IL-2) without additional cytokines. After 3 days, cells were harvested and analyzed by flow cytometry or Western blotting.

Lymphocyte staining and flow cytometry

Thymi, spleens, and mesenteric lymph nodes were minced into single-cell suspensions in phosphate-buffered saline (PBS), and splenocytes were depleted of red blood cells using ACK lysis buffer (homemade). For cell surface staining, cells were washed with staining buffer (2% FBS heat-inactivated in PBS with 1 mM EDTA and 0.1% sodium azide) and incubated with the indicated antibodies on ice for 30 min. Cells were washed two more times before being analyzed on a flow cytometer. For intracellular cytokine staining, cells were stimulated for 4 hours with PMA (phorbol 12-myristate-13-acetate; 50 ng/ml) and ionomycin (1 μg/ml; Sigma-Aldrich) in the presence of brefeldin A (5 μg/ml; BD Biosciences). Intracellular staining, including FoxP3 (FJK-16) was performed with the eBioscience Foxp3 staining buffer set (00-5523-00, eBioscience). For detection of phosphorylated signaling molecules, cells were serum-starved for 1 hour in serum-free RPMI 1640. Cells were stimulated with TGF-β (5 ng/ml; PeproTech), fixed with Phosflow Lyse/Fix buffer, followed by permeabilization with Phosflow Perm Buffer III (both from BD Biosciences), and stained with antibodies against P-SMAD2/3-APC (1:40 dilution; BD Biosciences). To determine expression of PCBP1, cell surface antigens were first stained before fix/perm with the FoxP3 staining buffer set (eBioscience, Thermo Fisher Scientific) and stained with Pcbp1 primary antibodies [followed by a fluorescein isothiocyanate–conjugated anti-rabbit immunoglobulin G (IgG) (BD Biosciences, USA)]. Expression of surface and intracellular markers was analyzed with a flow cytometer (BD FACSVerse) and FlowJo software (Tree Star Inc.).

Immunoblotting

T cells were stimulated under Th0 or iT_{reg} conditions as described previously (*21*). Th0 cells are defined as naïve $CD4^+$ T cells activated in the presence of anti-CD3/anti-CD28 antibodies and IL-2, but without TGF-β1, and maintained in complete T cell medium. Cells were harvested on day 3 or 4 and then counted and washed with cold serum-free RPMI 1640 medium. Cells were lysed with radioimmunoprecipitation assay buffer containing protease and phosphatase inhibitors and prepared for SDS–polyacrylamide gel electrophoresis. For immunoblotting, polyvinylidene difluoride membranes were blocked at room temperature for 1 hour with 6% nonfat milk blocking buffer and then probed with rabbit anti-PCBP1 and rabbit anti–phospho-PCBP1 (homemade), rabbit anti-moesin (Q480) and rabbit anti-eIF5A2 (D8L8Q) (Cell Signaling Technology), rat anti-FOXP3 (FJK-16s, eBioscience), rabbit anti–phospho-Smad3 (EP823Y) and rabbit anti-Smad3 (EP568Y) (both from Abcam), and mouse anti–β-actin (Sigma-Aldrich). Secondary anti-mouse (A8924), anti-rat (A5795), and anti-rabbit (A0545) IgG–horseradish peroxidase antibodies were obtained from Sigma-Aldrich.

RNA isolation, cDNA synthesis, and quantitative real-time polymerase chain reaction

Total RNA was isolated with RNeasy Plus kit (QIAGEN, CA), and cDNA was synthesized using the QuantiTect Reverse Transcription Kit (QIAGEN) according to the manufacturer's instructions or SuperScript reverse transcriptase reagent kit (Invitrogen). Quantitative polymerase chain reaction (PCR) was performed using SYBR Premix Ex Taq (Bio-Rad, USA) on a system (Life Technologies, USA). mRNA levels of *Pcbp1* and *Actb* were determined by the primers listed below. Gene expression was normalized to β-actin using the ΔΔCt. method (*Pcbp1*: forward, 5′-GGAAGAAAGGGGAGTCGGTG-3′ and reverse, 5′-AAGATGGCATTGGTAGGCCC-3′; *Actb*: forward, 5′-TTGCTGACAGGATGCAGAAG-3′ and reverse, 5′-ACATCTGCTGGAAGGTGGAC-3′).

RNA-seq and analysis

Total naïve $CD4^+$ T cells were isolated from the spleen of WT and *Pcbp1*$^{f/f}$ *Cd4*-Cre mice using the naïve T cell isolation kit (Miltenyi, USA). Total RNA was extracted from the cells and sent to Novogene for RNA-seq analysis. Libraries were prepared using 50 ng of total RNA using the NEBNext Ultra RNA Library Kit for Illumina (catalog no. E7530) and sequenced on HiSeq 3000 at 75 base pair paired-end. Each sample was analyzed in quadruplet. Sequencing reads were first evaluated for quality control using the FastQC software and then aligned against the mouse mm10 reference genome using the TopHat2 software. Mapped reads were assigned to gene features and quantified using the HTSeq software and further evaluated for quality control using correlation and multidimensional scaling plots. Normalization and differential expression were performed using the edgeR software. The significantly DEGs (FDR < 0.05) were visualized using heat maps and volcano plot representations and considered for subsequent functional enrichment analysis using ToppGene Suite.

Lentiviral production and transfection

Lentiviral particles were produced in HEK293FT cells according to standard protocols. Spleen-isolated primary $CD4^+CD25^-$ T cells (2×10^5 cells per well) were transduced with lentiviral supernatants. Murine lentiviral DNA plasmid against *Pcbp1* (hnRNP E1) (sequence: CCG GCC ATG ATC CAA CTG TGT AAT TCT CGA GAA TTA CAC AGT TGG ATC ATG GTT TTT G) (Sigma-Aldrich, TRC1-pLKO.1-puromycin) were transduced into $CD4^+$ T cells activated for 48 hours with anti-CD3 and anti-CD28 with polybrene (8 μg/ml; Sigma-Aldrich).

Diabetes model

Splenocytes from NOD mice were depleted of $CD25^+$ cells by incubating with anti-CD25 MACS beads (Miltenyi) and passing through the MACS LD column (Miltenyi). CD25-depleted splenocytes were adoptively transferred in recipient mice at 6×10^6 $CD25^-$ T cells per mouse, together with 2×10^5 scrambled, *Pcbp1* KD $CD4^+CD25^-$ T cells, or WT in vitro–induced T_{regs}, intravenously into NOD *Rag1*$^{-/-}$

mice. Blood glucose concentrations were then monitored kinetically. A glucose value of 200 mg/dl or more was defined as diabetic. Autoimmune destructions of pancreatic islet cells were verified by histology and insulin staining.

Histology

Mouse organs were fixed in 4% formalin, embedded in paraffin, sectioned, and stained following standard hematoxylin and eosin (H&E) staining protocol. For histology and multiplex cytokine assay, organs from KO and heterozygous mice were fixed with 3.7% formalin. After dehydration with 30% sucrose, tissues were then embedded in optimal cutting temperature compound, sectioned, and processed for H&E staining or insulin staining according to standard protocols.

Tumor models

WT or *Pcbp1*$^{f/f}$*Cd4-Cre* mice, aged 6 to 10 weeks, littermates were challenged subcutaneously with MC38 cells (1×10^6) or MB49 tumor cells (5×10^5). For all tumor models, tumors were measured regularly with a caliper by personnel blinded to the genotype of the mice. Tumor area was calculated using the equation ($L \times W$), where L denotes length and W denotes width. The maximal tumor burden was 400 mm^2, and this limit was not exceeded in any of the experiments. Tumor-bearing mice were euthanized at 20 days after inoculation and harvested for TIL analysis. In all flow cytometry experiments, tumors of similar sizes were used for comparison. All animals were housed under specific pathogen–free conditions in accordance with institutional and federal guidelines.

Study design

The aim of this study was to characterize the roles of PCBP1 in effector T cell functions. The studies were performed using groups of age- and gender-matched mice, 6 to 10 weeks old. We generated a Pcbp1 conditional KO mouse model (*Pcbp1*$^{fl/fl}$*Cd4*-Cre) and tested their responses against *Pcbp1*$^{+/+}$*Cd4*-Cre littermate controls. The number of replicates for each experiment is indicated in the figure legends. No animals were excluded in the studies. Histological analyses were performed double-blinded where appropriate.

GVHD model in vivo

Major histocompatibility complex–mismatched (B6 → BALB/c) BMT model was used as previously established. Briefly, recipient BALB/c mice (7 to 8 weeks old) were conditioned with total body irradiation at 700 centigray (single dose) using X-RAD 320 irradiators (Precision X-ray Inc., North Branford, CT). Within 24 hours after irradiation, recipients were intravenously injected with 5×10^6 TCD BM alone or with 7×10^5 T cells (CD25$^+$ depleted) from WT or KO, which were purified from the spleen and lymph node by negative depletion using magnetic beads as previously described (*35*). Recipient mice were monitored for survival, body weight loss, and GVHD clinical score for 80 days. The GVHD clinical scores were tabulated as five parameters: weight loss, posture, activity, fur texture, and skin integrity.

Statistical analyses

Statistical parameters are all reported in the figure legends. Statistical analyses were performed with Prism software version 5.0 or 8.0 (GraphPad Software, La Jolla, CA, USA; https://graphpad.com), and significances were determined using Student's t test, one-way analysis of variance (ANOVA), log-rank test, and Mann-Whitney nonparametric test where specified. All data are presented as means ± SE or SD unless otherwise stated. All experiments were carried out in triplicate technical and biological replicates unless otherwise stated. *$P < 0.05$, **$P < 0.01$, ***$P < 0.001$, and ****$P < 0.0001$ were considered to be statistically significant.

SUPPLEMENTARY MATERIALS

Supplementary material for this article is available at http://advances.sciencemag.org/cgi/content/full/6/22/eaaz3865/DC1

View/request a protocol for this paper from *Bio-protocol*.

REFERENCES AND NOTES

1. P. Sharma, J. P. Allison, Immune checkpoint targeting in cancer therapy: Toward combination strategies with curative potential. *Cell* **161**, 205–214 (2015).
2. Z. Li, W. Song, M. Rubinstein, D. Liu, Recent updates in cancer immunotherapy: A comprehensive review and perspective of the 2018 China Cancer Immunotherapy Workshop in Beijing. *J. Hematol. Oncol.* **11**, 142 (2018).
3. M. F. Sanmamed, L. Chen, A paradigm shift in cancer immunotherapy: From enhancement to normalization. *Cell* **175**, 313–326 (2018).
4. K. Chamoto, M. Al-Habsi, T. Honjo, Role of PD-1 in immunity and diseases. *Curr. Top. Microbiol. Immunol.* **410**, 75–97 (2017).
5. T. N. Gide, C. Quek, A. M. Menzies, A. T. Tasker, P. Shang, J. Holst, J. Madore, S. Y. Lim, R. Velickovic, M. Wongchenko, Y. Yan, S. Lo, M. S. Carlino, A. Guminski, R. P. M. Saw, A. Pang, H. M. McGuire, U. Palendira, J. F. Thompson, H. Rizos, I. P. D. Silva, M. Batten, R. A. Scolyer, G. V. Long, J. S. Wilmott, Distinct immune cell populations define response to anti-PD-1 monotherapy and anti-PD-1/anti-CTLA-4 combined therapy. *Cancer Cell* **35**, 238–255.e6 (2019).
6. D. Davar, J. M. Kirkwood, PD-1 immune checkpoint inhibitors and immune-related adverse events: Understanding the upside of the downside of checkpoint blockade. *JAMA Oncol.* **5**, 942–943 (2019).
7. T. Kamada, Y. Togashi, C. Tay, D. Ha, A. Sasaki, Y. Nakamura, E. Sato, S. Fukuoka, Y. Tada, A. Tanaka, H. Morikawa, A. Kawazoe, T. Kinoshita, K. Shitara, S. Sakaguchi, H. Nishikawa, PD-1$^+$ regulatory T cells amplified by PD-1 blockade promote hyperprogression of cancer. *Proc. Natl. Acad. Sci. U.S.A.* **116**, 9999–10008 (2019).
8. M. Turner, M. D. Díaz-Muñoz, RNA-binding proteins control gene expression and cell fate in the immune system. *Nat. Immunol.* **19**, 120–129 (2018).
9. P. Techasintana, J. S. Ellis, J. Glascock, M. M. Gubin, S. E. Ridenhour, J. D. Magee, M. L. Hart, P. Yao, H. Zhou, M. S. Whitney, C. L. Franklin, J. L. Martindale, M. Gorospe, W. J. Davis, P. L. Fox, X. Li, U. Atasoy, The RNA-binding protein HuR posttranscriptionally regulates IL-2 homeostasis and CD4$^+$ Th2 differentiation. *Immunohorizons* **1**, 109–123 (2017).
10. K. U. Vogel, L. S. Bell, A. Galloway, H. Ahlfors, M. Turner, The RNA-binding proteins Zfp36l1 and Zfp36l2 enforce the thymic β-selection checkpoint by limiting DNA damage response signaling and cell cycle progression. *J. Immunol.* **197**, 2673–2685 (2016).
11. S. Leidgens, K. Z. Bullough, H. Shi, F. Li, M. Shakoury-Elizeh, T. Yabe, P. Subramanian, E. Hsu, N. Natarajan, A. Nandal, T. L. Stemmler, C. C. Philpott, Each member of the poly-r(C)-binding protein 1 (PCBP) family exhibits iron chaperone activity toward ferritin. *J. Biol. Chem.* **288**, 17791–17802 (2013).
12. M. S. Ryu, D. Zhang, O. Protchenko, M. Shakoury-Elizeh, C. C. Philpott, PCBP1 and NCOA4 regulate erythroid iron storage and heme biosynthesis. *J. Clin. Invest.* **127**, 1786–1797 (2017).
13. C. C. Philpott, M. S. Ryu, A. Frey, S. Patel, Cytosolic iron chaperones: Proteins delivering iron cofactors in the cytosol of mammalian cells. *J. Biol. Chem.* **292**, 12764–12771 (2017).
14. X. Ji, J. Humenik, D. Yang, S. A. Liebhaber, PolyC-binding proteins enhance expression of the CDK2 cell cycle regulatory protein via alternative splicing. *Nucleic Acids Res.* **46**, 2030–2044 (2018).
15. V. Tripathi, K. M. Sixt, S. Gao, X. Xu, J. Huang, R. Weigert, M. Zhou, Y. E. Zhang, Direct regulation of alternative splicing by SMAD3 through PCBP1 is essential to the tumor-promoting role of TGF-β. *Mol. Cell* **64**, 1010 (2016).
16. C. K. Hwang, Y. Wagley, P. Y. Law, L. N. Wei, H. H. Loh, Phosphorylation of poly(rC) binding protein 1 (PCBP1) contributes to stabilization of mu opioid receptor (MOR) mRNA via interaction with AU-rich element RNA-binding protein 1 (AUF1) and poly A binding protein (PABP). *Gene* **598**, 113–130 (2017).
17. B. V. Howley, P. H. Howe, TGF-beta signaling in cancer: Post-transcriptional regulation of EMT via hnRNP E1. *Cytokine* **118**, 19–26 (2018).
18. A. Chaudhury, G. S. Hussey, P. S. Ray, G. Jin, P. L. Fox, P. H. Howe, TGF-β-mediated phosphorylation of hnRNP E1 induces EMT via transcript-selective translational induction of Dab2 and ILEI. *Nat. Cell Biol.* **12**, 286–293 (2010).
19. G. S. Hussey, A. Chaudhury, A. E. Dawson, D. J. Lindner, C. R. Knudsen, M. C. J. Wilce, W. C. Merrick, P. H. Howe, Identification of an mRNP complex regulating tumorigenesis at the translational elongation step. *Mol. Cell* **41**, 419–431 (2011).

20. G. S. Hussey, L. A. Link, A. S. Brown, B. V. Howley, A. Chaudhury, P. H. Howe, Establishment of a TGFβ-induced post-transcriptional EMT gene signature. *PLOS ONE* **7**, e52624 (2012).
21. E. A. Ansa-Addo, Y. Zhang, Y. Yang, G. S. Hussey, B. V. Howley, M. Salem, B. Riesenberg, S. Sun, D. C. Rockey, S. Karvar, P. H. Howe, B. Liu, Z. Li, Membrane-organizing protein moesin controls Treg differentiation and antitumor immunity via TGF-β signaling. *J. Clin. Invest.* **127**, 1321–1337 (2017).
22. Z. Wang, W. Yin, L. Zhu, J. Li, Y. Yao, F. Chen, M. Sun, J. Zhang, N. Shen, Y. Song, X. Chang, Iron drives T helper cell pathogenicity by promoting RNA-binding protein PCBP1-mediated proinflammatory cytokine production. *Immunity* **49**, 80–92.e7 (2018).
23. D. R. Fernandez, T. Telarico, E. Bonilla, Q. Li, S. Banerjee, F. A. Middleton, P. E. Phillips, M. K. Crow, S. Oess, W. Muller-Esterl, A. Perl, Activation of mammalian target of rapamycin controls the loss of TCRzeta in lupus T cells through HRES-1/Rab4-regulated lysosomal degradation. *J. Immunol.* **182**, 2063–2073 (2009).
24. L. R. Ghanem, A. Kromer, I. M. Silverman, P. Chatterji, E. Traxler, A. Penzo-Mendez, M. J. Weiss, B. Z. Stanger, S. A. Liebhaber, The Poly(C) binding protein Pcbp2 and its retrotransposed derivative Pcbp1 are independently essential to mouse development. *Mol. Cell. Biol.* **36**, 304–319 (2016).
25. C. W. Lio, C. S. Hsieh, A two-step process for thymic regulatory T cell development. *Immunity* **28**, 100–111 (2008).
26. N. Sugimoto, T. Oida, K. Hirota, K. Nakamura, T. Nomura, T. Uchiyama, S. Sakaguchi, Foxp3-dependent and -independent molecules specific for CD25+CD4+ natural regulatory T cells revealed by DNA microarray analysis. *Int. Immunol.* **18**, 1197–1209 (2006).
27. J. M. Weiss, A. M. Bilate, M. Gobert, Y. Ding, M. A. Curotto de Lafaille, C. N. Parkhurst, H. Xiong, J. Dolpady, A. B. Frey, M. G. Ruocco, Y. Yang, S. Floess, J. Huehn, S. Oh, M. O. Li, R. E. Niec, A. Y. Rudensky, M. L. Dustin, D. R. Littman, J. J. Lafaille, Neuropilin 1 is expressed on thymus-derived natural regulatory T cells, but not mucosa-generated induced Foxp3+ T reg cells. *J. Exp. Med.* **209**, 1723–1742 (2012).
28. Y. Kitagawa, N. Ohkura, Y. Kidani, A. Vandenbon, K. Hirota, R. Kawakami, K. Yasuda, D. Motooka, S. Nakamura, M. Kondo, I. Taniuchi, T. Kohwi-Shigematsu, S. Sakaguchi, Guidance of regulatory T cell development by Satb1-dependent super-enhancer establishment. *Nat. Immunol.* **18**, 173–183 (2017).
29. E. Tu, C. P. Z. Chia, W. Chen, D. Zhang, S. A. Park, W. Jin, D. Wang, M. L. Alegre, Y. E. Zhang, L. Sun, W. J. Chen, T cell receptor-regulated TGF-β type I receptor expression determines T cell quiescence and activation. *Immunity* **48**, 745–759.e6 (2018).
30. W. Chen, J. E. Konkel, Development of thymic Foxp3^{+} regulatory T cells: TGF-β matters. *Eur. J. Immunol.* **45**, 958–965 (2015).
31. J. E. Konkel, D. Zhang, P. Zanvit, C. Chia, T. Zangarle-Murray, W. Jin, S. Wang, W. J. Chen, Transforming growth Factor-β signaling in regulatory T cells controls T helper-17 cells and tissue-specific immune responses. *Immunity* **46**, 660–674 (2017).
32. B. C. Betts, D. Bastian, S. Iamsawat, H. Nguyen, J. L. Heinrichs, Y. Wu, A. Daenthanasanmak, A. Veerapathran, A. O'Mahony, K. Walton, J. Reff, P. Horna, E. M. Sagatys, M. C. Lee, J. Singer, Y. J. Chang, C. Liu, J. Pidala, C. Anasetti, X. Z. Yu, Targeting JAK2 reduces GVHD and xenograft rejection through regulation of T cell differentiation. *Proc. Natl. Acad. Sci. U.S.A.* **115**, 1582–1587 (2018).
33. C. Fondi, C. Nozzoli, S. Benemei, G. Baroni, R. Saccardi, S. Guidi, P. Nicoletti, B. Bartolozzi, N. Pimpinelli, M. Santucci, A. Bosi, D. Massi, Increase in FOXP3+ regulatory T cells in GVHD skin biopsies is associated with lower disease severity and treatment response. *Biol. Blood Marrow Transplant.* **15**, 938–947 (2009).
34. A. Daenthanasanmak, S. Iamsawat, P. Chakraborty, H. D. Nguyen, D. Bastian, C. Liu, S. Mehrotra, X. Z. Yu, Targeting Sirt-1 controls GVHD by inhibiting T-cell allo-response and promoting Treg stability in mice. *Blood* **133**, 266–279 (2019).
35. S. Iamsawat, A. Daenthanasanmak, J. H. Voss, H. Nguyen, D. Bastian, C. Liu, X. Z. Yu, Stabilization of Foxp3 by targeting JAK2 enhances efficacy of CD8 induced regulatory T cells in the prevention of Graft-versus-Host disease. *J. Immunol.* **201**, 2812–2823 (2018).
36. M. Leclerc, S. Naserian, C. Pilon, A. Thiolat, G. H. Martin, C. Pouchy, C. Dominique, Y. Belkacemi, F. Charlotte, S. Maury, B. L. Salomon, J. L. Cohen, Control of GVHD by regulatory T cells depends on TNF produced by T cells and TNFR2 expressed by regulatory T cells. *Blood* **128**, 1651–1659 (2016).
37. H. Wang, Y. G. Yang, The complex and central role of interferon-γ in graft-versus-host disease and graft-versus-tumor activity. *Immunol. Rev.* **258**, 30–44 (2014).
38. K. Aida, R. Miyakawa, K. Suzuki, K. Narumi, T. Udagawa, Y. Yamamoto, T. Chikaraishi, T. Yoshida, K. Aoki, Suppression of Tregs by anti-glucocorticoid induced TNFreceptor antibody enhances the antitumor immunity of interferon-α gene therapy for pancreatic cancer. *Cancer Sci.* **105**, 159–167 (2014).
39. R. M. Samstein, A. Arvey, S. Z. Josefowicz, X. Peng, A. Reynolds, R. Sandstrom, S. Neph, P. Sabo, J. M. Kim, W. Liao, M. O. Li, C. Leslie, J. A. Stamatoyannopoulos, A. Y. Rudensky, Foxp3 exploits a pre-existent enhancer landscape for regulatory T cell lineage specification. *Cell* **151**, 153–166 (2012).
40. G. S. Hussey, B. V. Howley, P. H. Howe, Post-transcriptional mapping reveals critical regulators of metastasis. *Oncoscience* **2**, 831–832 (2015).
41. S. Rachidi, A. Metelli, B. Riesenberg, B. X. Wu, M. H. Nelson, C. Wallace, C. M. Paulos, M. P. Rubinstein, E. Garrett-Mayer, M. Hennig, D. W. Bearden, Y. Yang, B. Liu, Z. Li, Platelets subvert T cell immunity against cancer via GARP-TGFβ axis. *Sci Immunol.* **2**, eaai7911 (2017).
42. X. Tai, B. Erman, A. Alag, J. Mu, M. Kimura, G. Katz, T. Guinter, T. McCaughtry, R. Etzensperger, L. Feigenbaum, D. S. Singer, A. Singer, Foxp3 transcription factor is proapoptotic and lethal to developing regulatory T cells unless counterbalanced by cytokine survival signals. *Immunity* **38**, 1116–1128 (2013).
43. W. Hugo, J. M. Zaretsky, L. Sun, C. Song, B. H. Moreno, S. Hu-Lieskovan, B. Berent-Maoz, J. Pang, B. Chmielowski, G. Cherry, E. Seja, S. Lomeli, X. Kong, M. C. Kelley, J. A. Sosman, D. B. Johnson, A. Ribas, R. S. Lo, Genomic and transcriptomic features of response to Anti-PD-1 therapy in metastatic melanoma. *Cell* **165**, 35–44 (2016).
44. J. D. Fontenot, M. A. Gavin, A. Y. Rudensky, Foxp3 programs the development and function of CD4+CD25+ regulatory T cells. *Nat. Immunol.* **4**, 330–336 (2003).
45. S. Hori, T. Nomura, S. Sakaguchi, Control of regulatory T cell development by the transcription factor Foxp3. *Science* **299**, 1057–1061 (2003).
46. C. Govindaraj, K. Scalzo-Inguanti, M. Madondo, J. Hallo, K. Flanagan, M. Quinn, M. Plebanski, Impaired Th1 immunity in ovarian cancer patients is mediated by TNFR2+ Tregs within the tumor microenvironment. *Clin. Immunol.* **149**, 97–110 (2013).
47. R. Roychoudhuri, R. L. Eil, D. Clever, C. A. Klebanoff, M. Sukumar, F. M. Grant, Z. Yu, G. Mehta, H. Liu, P. Jin, Y. Ji, D. C. Palmer, J. H. Pan, A. Chichura, J. G. Crompton, S. J. Patel, D. Stroncek, E. Wang, F. M. Marincola, K. Okkenhaug, L. Gattinoni, N. P. Restifo, The transcription factor BACH2 promotes tumor immunosuppression. *J. Clin. Invest.* **126**, 599–604 (2016).
48. R. Newman, J. McHugh, M. Turner, RNA binding proteins as regulators of immune cell biology. *Clin. Exp. Immunol.* **183**, 37–49 (2016).
49. M. Turner, E. Monzón-Casanova, RNA-binding proteins mind the GAPs. *Nat. Immunol.* **18**, 146–148 (2017).
50. J. Guo, R. Jia, Splicing factor poly(rC)-binding protein 1 is a novel and distinctive tumor suppressor. *J. Cell. Physiol.* **234**, 33–41 (2018).
51. M. Zhou, X. Tong, Downregulated Poly-C binding protein-1 is a novel predictor associated with poor prognosis in acute myeloid leukemia. *Diagn. Pathol.* **10**, 147 (2015).
52. J. Fu, D. Wang, Y. Yu, J. Heinrichs, Y. Wu, S. Schutt, K. Kaosaard, C. Liu, K. Haarberg, D. Bastian, D. G. McDonald, C. Anasetti, X. Z. Yu, T-bet is critical for the development of acute graft-versus-host disease through controlling T cell differentiation and function. *J. Immunol.* **194**, 388–397 (2014).
53. R. Roychoudhuri, K. Hirahara, K. Mousavi, D. Clever, C. A. Klebanoff, M. Bonelli, G. Sciumè, H. Zare, G. Vahedi, B. Dema, Z. Yu, H. Liu, H. Takahashi, M. Rao, P. Muranski, J. G. Crompton, G. Punkosdy, D. Bedognetti, E. Wang, V. Hoffmann, J. Rivera, F. M. Marincola, A. Nakamura, V. Sartorelli, Y. Kanno, L. Gattinoni, A. Muto, K. Igarashi, J. J. O'Shea, N. P. Restifo, BACH2 represses effector programs to stabilize T_{reg}-mediated immune homeostasis. *Nature* **498**, 506–510 (2013).
54. W. Pan, S. Zhu, D. Dai, Z. Liu, D. Li, B. Li, N. Gagliani, Y. Zheng, Y. Tang, M. T. Weirauch, X. Chen, W. Zhu, Y. Wang, B. Chen, Y. Qian, Y. Chen, J. Fang, R. Herbst, L. Richman, B. Jallal, J. B. Harley, R. A. Flavell, Y. Yao, N. Shen, MiR-125a targets effector programs to stabilize Treg-mediated immune homeostasis. *Nat. Commun.* **6**, 7096 (2015).
55. J. C. Fischer, V. Otten, M. Kober, C. Drees, M. Rosenbaum, M. Schmickl, S. Heidegger, R. Beyaert, G. van Loo, X. C. Li, C. Peschel, M. Schmidt-Supprian, T. Haas, S. Spoerl, H. Poeck, A20 restrains thymic regulatory T cell development. *J. Immunol.* **199**, 2356–2365 (2017).
56. A. Galloway, A. Saveliev, S. ukasiak, D. J. Hodson, D. Bolland, K. Balmanno, H. Ahlfors, E. Monzon-Casanova, S. C. Mannurita, L. S. Bell, S. Andrews, M. D. Diaz-Munoz, S. J. Cook, A. Corcoran, M. Turner, RNA-binding proteins ZFP36L1 and ZFP36L2 promote cell quiescence. *Science* **352**, 453–459 (2016).
57. M. D. Diaz-Muñoz, S. E. Bell, K. Fairfax, E. Monzon-Casanova, A. F. Cunningham, M. Gonzalez-Porta, S. R. Andrews, V. I. Bunik, K. Zarnack, T. Curk, W. A. Heggermont, S. Heymans, G. E. Gibson, D. L. Kontoyiannis, J. Ule, M. Turner, The RNA-binding protein HuR is essential for the B cell antibody response. *Nat. Immunol.* **16**, 415–425 (2015).
58. Y. Zhang, B. X. Wu, A. Metelli, J. E. Thaxton, F. Hong, S. Rachidi, E. Ansa-Addo, S. Sun, C. Vasu, Y. Yang, B. Liu, Z. Li, GP96 is a GARP chaperone and controls regulatory T cell functions. *J. Clin. Invest.* **125**, 859–869 (2015).

Acknowledgments: We thank A. Henderson (Ansa-Addo Lab) and members of the Li, Liu, and Howe laboratories for assistance and insightful discussions on the project. We also thank O. Protchenko in the Philpott laboratory for help in obtaining the *Pcbp1*-flox mice. We also thank members of the Pelotonia Institute for Immuno-Oncology at Ohio State University (OSU) and the Cancer Immunology Program at the Hollings Cancer Center (MUSC) for helpful discussions. **Funding:** This research was supported by the NIH R01CA188419, R01AI070603, and P01CA186866 (to Z.L.), the American Cancer Society Intra-institutional Grant 129806-IRG-16-185-17-IRG (to E.A.A.-A.), and the Flow Cytometry & Cell Sorting Shared Resource Unit at the OSU and Hollings Cancer Center. **Author contributions:** E.A.A.-A. and Z.L. designed and

oversaw the study. E.A.A.-A., H.-C.H., B.R., S.I., D.B., and M.H.N. performed experiments and data analysis. J.H.N. and D.C. analyzed RNA-seq data and generated graphs. C.M.P., B.L., X.-Z.Y., C.P., and P.H.H. provided reagents and expertise in experimental design and data interpretation. E.A.A.-A. and Z.L. wrote the manuscript with input from all coauthors. **Competing interests:** The authors declare that they have no competing interests. **Data and materials availability:** RNA-seq data have been deposited in the GEO database under accession number GSE131826. The *Pcbp1* mutant mouse strain is available through a material transfer agreement with OSU. Requests for mice should be directed to Z.L. All other data needed to evaluate the conclusions in the paper are present in the paper and/or the Supplementary Materials.

Submitted 4 September 2019
Accepted 25 March 2020
Published 29 May 2020
10.1126/sciadv.aaz3865

Citation: E. A. Ansa-Addo, H.-C. Huang, B. Riesenberg, S. Iamsawat, D. Borucki, M. H. Nelson, J. H. Nam, D. Chung, C. M. Paulos, B. Liu, X.-Z. Yu, C. Philpott, P. H. Howe, Z. Li, RNA binding protein PCBP1 is an intracellular immune checkpoint for shaping T cell responses in cancer immunity. *Sci. Adv.* **6**, eaaz3865 (2020).